

DEFORESTATION ANALYSIS USING REMOTE SENSING

By

NEBYU YONAS SUTRI

DISSERTATION

Submitted to the Electrical & Electronics Engineering Programme

in Partial Fulfillment of the Requirements

for the Degree

Bachelor of Engineering (Hons)

(Electrical & Electronics Engineering)

May, 2011

Universiti Teknologi Petronas

Bandar Seri Iskandar

31750 Tronoh

Perak Darul Ridzuan

CERTIFICATION OF APPROVAL

DEFORESTATION ANALYSIS USING REMOTE SENSING

by

Nebyu Yonas Sutri

A project dissertation submitted to the

Electrical and Electronics Engineering Programme

Universiti Teknologi PETRONAS

in partial fulfilment of the requirement for the

BACHELOR OF ENGINEERING (Hons)

(ELECTRICAL AND ELECTRONICS ENGINEERING)

Approved by,



(Dr. Aamir Saeed Malik)

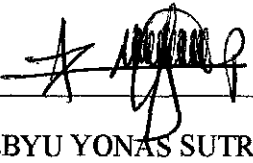
UNIVERSITI TEKNOLOGI PETRONAS

TRONOH, PERAK

May, 2011

CERTIFICATION OF ORIGINALITY

This is to certify that I am responsible for the work submitted in this project, that the original work is my own except as specified in the references and acknowledgements, and that the original work contained herein have not been undertaken or done by unspecified sources or persons.



NEBYU YONAS SUTRI

ABSTRACT

Deforestation is becoming a great danger to the existence of our mother world, Earth, in recent years. Clearance and removal of trees without sufficient replacement resulted in a wide range change of forestlands all over the world. Because of that forest qualities are being degraded continuously, plant and animal lives are being affected negatively. Deforestation also imposed its negative impact on soil, climate and environment.

Population expansion, industrialization and scarcity of land are the major causes for the deforestation. However economical and natural reasons like, dependences for heat and energy, wildfire and drought also contribute for the aggravation of this problem. Deforestation affects human life and environment in a negative way. Therefore it is a global desire to come up with a structured way of checking, monitoring and fighting this great danger worldwide before it is too late to take things back to order.

This project presents a fuzzy c-mean clustering segmentation based deforestation analysis using remotely sensed data. Remote sensing has given a very unique and reliable source of data for forestation and deforestation monitoring and which can be extracted easily, cheaply and timely. This study gives an analysis of OTSU and Fuzzy c-mean segmentation based effective deforestation analysis methods which deploy satellite images to study and analyze deforestation rates.

ACKNOWLEDGEMENT

Before saying anything I would like to thank **GOD** for His grace and Mercy that He gave me to get through this project. I would like to take this opportunity to thank all parties who has contributed their effort for the completion of this project.

I would like to express my most sincere and deepest appreciation to my supervisor Dr. Aamir Saeed Malik for providing me the opportunity to be supervised under him and providing me all the necessary information and materials for this project, I am thankful for his limitless support and supervision.

I would like to express my deepest gratitude to all staff of *Electrical and Electronics Engineering Department* at Universiti Teknologi PETRONAS, especially Final Year Project I and II coordinators and Computer Vision and Image Processing graduate assistants. I am thankful to them for their kind cooperation's and help.

The greatest appreciation goes to my family who did everything for me from the moment I was born to the present. I would not be a person who I have become today without their help and positive attitude towards me. Furthermore, I would like to thank my friends for their comments, help and positive criticism.

TABLE CONTENTS

CHAPTER 1.....	1
INTRODUCTION.....	1
1.1 Background of study.....	1
1.2 Problem statement.....	3
1.3 Objective and scope of project.....	3
CHAPTER 2.....	5
LITERATURE REVIEW.....	5
2.1 Remote sensing.....	5
2.2 Deforestation in relation to human population.....	7
2.3 Color spaces.....	10
2.3.1 L*a*b* color space.....	10
2.3.2 HSV and HSI color spaces.....	11
CHAPTER 3.....	13
METHODOLOGY.....	13
3.1 Data Acquisitions.....	13
3.2 Feature selection.....	13
3.3 Satellite (Digital) image processing.....	14
3.3.1 Image Segmentation, Otsu method.....	14
3.3.2 Image clustering.....	15
3.4 Tools and equipment used.....	17
CHAPTER 4.....	18
RESULTS AND DISCUSSION.....	18
4.1 Color space transformations and feature selections.....	18
4.2 Deforestation analysis algorithms implementation and analysis.....	22
4.2.1 Ground truth data.....	23

4.2.2	OTSU segmentation and Fuzzy c-means clustering.....	24
4.3	Accuracy assessment	25
4.4	Comparison between Fuzzy c-mean clustering and OTSU segmentation	30
4.5	Application of Fuzzy C-mean clustering in selected images	32
4.6	Real case scenario application of the Fuzzy c-mean clustering.....	32
4.6.1	Future deforestation prediction of Rodonia.....	35
CHAPTER 5	37
CONCLUSION AND RECOMMENDATION	37
REFERENCES	39
Appendix A	A
Appendix B	B
Appendix C	C
Appendix D	F
Appendix E	H
Appendix F	J
Appendix G	N
Appendix H	R

LIST OF TABLES

Table 1: Deforestation prediction by the year 2050 [9] 8

Table 2: Agents of deforestation and their responsible region [3] 9

Table 3 : Fuzzy c-mean clustering result 26

Table 4: Otsu segmentation result 26

Table 5: fcm and Otsu comparison 30

Table 6: fcm clustering results 32

Table 7: Percentage of deforested area computed 35

LIST OF FIGURES

Figure 1: Deforestation in Malaysian Borneo (source NASA images [19]) 2

Figure 2: Deforestation in RONDONIA, BRAZIL (source NASA images [19])... 2

Figure 3: Satellite image of Malaysia (source NASA images [19]) 4

Figure 4: High resolution satellite image of Amazon (source NASA images [19]) 4

Figure 5 : Russia wildfire, 2010 (Source CNN news [10]) 6

Figure 6: Forest coverage prediction 1990 – 2050 [9] 8

Figure 7 : Causes of deforestations [3]..... 10

Figure 8: HSI and HSV color spaces 12

Figure 9: Tools used 17

Figure 10: L*a*b* color space transformation 19

Figure 11: L*a*b* color space OTSU segmentation 19

Figure 12: HSV color space transformation..... 20

Figure 13 : HSV color space OTSU segmentation 20

Figure 14: HSI color space transformation 21

Figure 15: HSI color space OTSU segmentation 21

Figure 16 : Ground truth data for 1975 23

Figure 17: Ground truth data for 1989 23

Figure 18: Ground truth data for 2001 24

Figure 19: 1975 RMSE and correlation FCM..... 27

Figure 20: 1989 RMSE and correlation FCM..... 27

Figure 21: 2001 RMSE and correlation FCM..... 28

Figure 22: 1975 RMSE and correlation OTSU 28

Figure 23: 1989 RMSE and correlation OTSU 29

Figure 24: 2001 RMSE and correlation OTSU 29

Figure 25: Correlation comparison of fcm and Otsu..... 31

Figure 26: RMSE comparison of fcm and Otsu 31

Figure 27: 1975 original versus fcm segmented image..... 34

Figure 28: 1989 original versus fcm segmented image..... 34

Figure 29: 2001 original versus fcm segmented image..... 34

Figure 30: Deforestation prediction for Rodonia, Brazil 36

CHAPTER 1

INTRODUCTION

1.1 Background of study

Forests like other natural resources have been continuously exploited and used by human beings since dawn of human history. There are many factors which contributed for deforestation. However most of the reasons are directly related to population expansion which resulted in change of forest lands to mechanized farmlands, pastures, mines and urban. Further human civilization and the 18th and 19th century industrial revolution, resulted major changes in settlement, agriculture, constructions and mining which increased the demand of trees wood industries and large scale farming, which further aggravated deforestation problem and forced the conversion of many forestlands to non-forest.

Further in Africa, Latin America and part of Asia, due to dependency of the population on wood and trees for heat and energy uses cleared considerable hectares of trees every year. In addition intentional or unintentional wildfires, environmental pollutions, natural disasters like droughts and earthquakes and increased consumption of trees resulted degradation in forest qualities. [1]

All the above mentioned causes affected the forestland all over the world and consequently affected soil, environment, vegetation and human lives. Which in turn resulted soil erosion, water contamination and in general reduction of life quality and global warming.

There are a wide range of definitions for deforestation, according to Wikipedia, Encyclopedia, deforestation is a cutting, burning or removing of forests for any other purposes of interest. Whereas, a much broader definition for deforestation is given by Food and Agriculture Organization of the United Nation (FAO of UN). According to FAO of UN, deforestation do not only include cutting down or

removing of tress but any activities which result in changing of forestland to other uses like farming, mining, construction etc. Based on the wider definition deforestation is and activity resulting in the reduction of the forest quality or reduction of tree cover below the 10% threshold.[3]

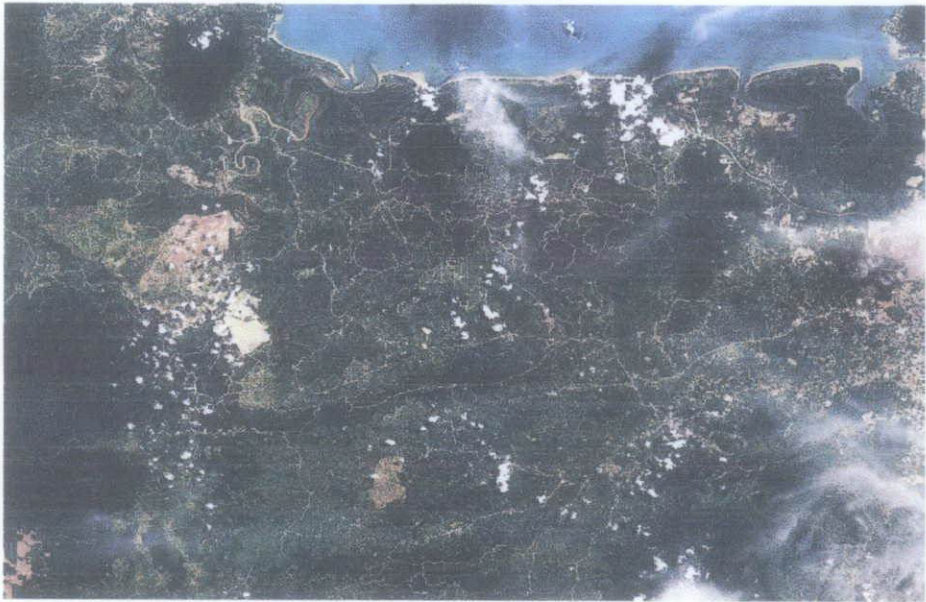


Figure 1: Deforestation in Malaysian Borneo (source NASA images [19])

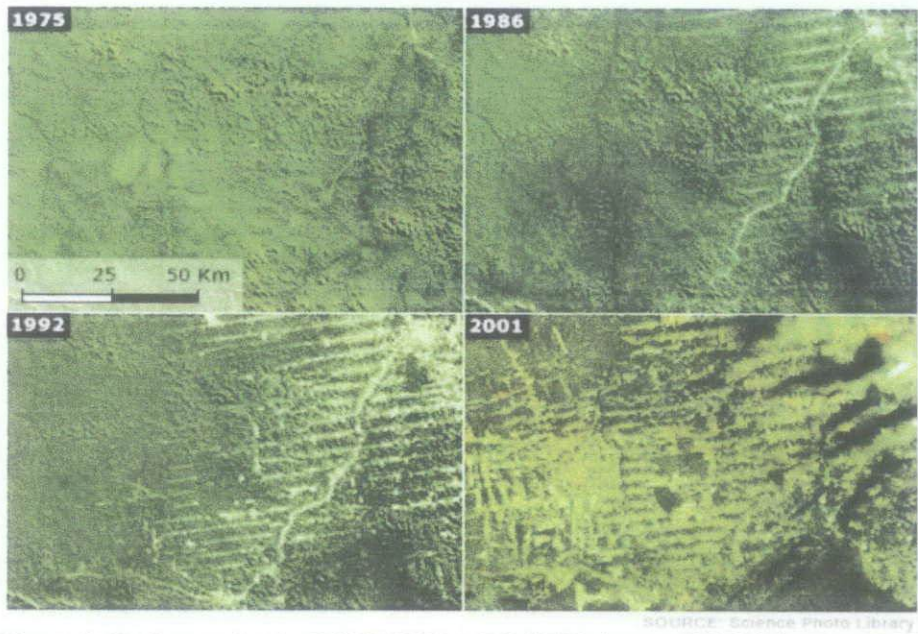


Figure 2: Deforestation in RONDONIA, BRAZIL (source NASA images [19])

1.2 Problem statement

Deforestation has been going on for centuries without sufficient monitoring and attempts to control the rate. Deforestation had been influencing plant and animal lives and the world at large. Researches and studies conducted [5, 9, 4, 11] on deforestations verify that deforestation is at alarming stage and needs urgent attention and coordinated responses.

Deforestation is responsible for Greenhouse gas and carbon di-oxide emissions and hence major factor of global warming and its aftermaths [4]. Hence it becomes no more regional issue but global problem which affects all regions of the world, which has affected and being affecting all regions of the world.

Prolonged and uncontrolled deforestations of forest lands put many plant and animal lives in danger of extinctions and changes like, desertification and climate changes. Human activities has highly affected forest environments and forced about 40% of world forests to be changed to less diversified and less dense forests or cleared totally [5].

But unfortunately, there is no unique or single worldwide deforestation analysis and fighting mechanism. Therefore it is definite that effective monitoring of forests is required in order to check deforestation and control the rate and ensure continuity of plant and animal life. Hence so many researches and studies are being carried on deforestation analysis which could assist human beings to cope with the dangers deforestation shatters.

1.3 Objective and scope of project

The objective of this project is to study and implement various algorithms for deforestation analysis using remote sensing data, like satellite imaging. It aimed at delivering a software module for assessment of deforestation. Though

deforestation is a global problem due to time, data and budget constraints the analysis is restricted to a specific area, Rodonia Brazil, Amazon forest, which can be expanded and used to analyze and study deforestation rates around the world (Please refer figure 3 and 4 below).



Figure 3: Satellite image of Malaysia (source NASA images [19])

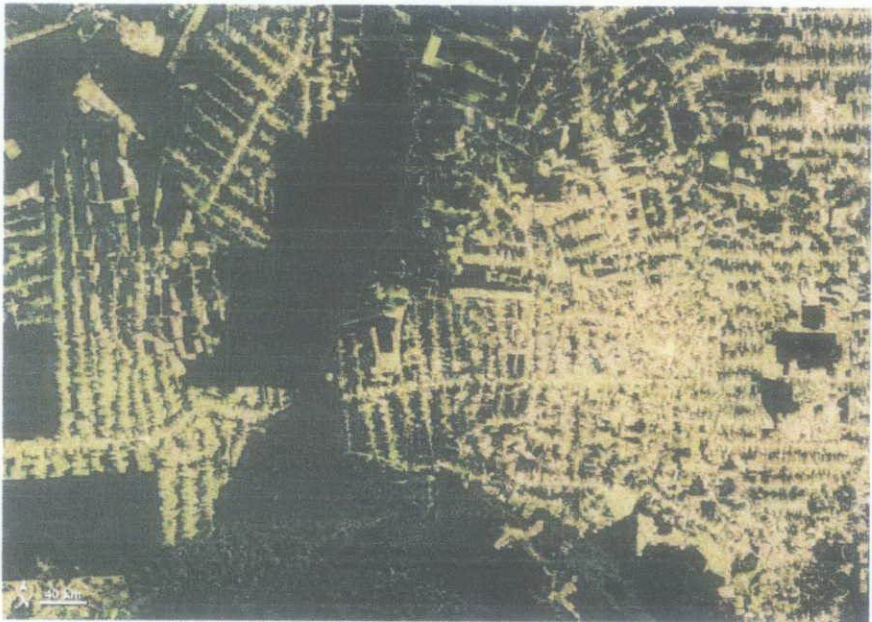


Figure 4: High resolution satellite image of Amazon (source NASA images [19])

CHAPTER 2

LITERATURE REVIEW

2.1 Remote sensing

Remote sensing is an activity in which we collect information and data about an object or area under study by using a device which is not in contact with the area or object under study [6]. Simplicity of getting remotely sensed data makes deforestation or forest land change monitoring and study possible for any given period of time. Further remotely sensed data can be acquired timely and easily compared to field data collection, which makes it more reliable and dependable source.[2]

There are many advantages remote sensing offers, first remotely sensed data can be obtained chronologically in different time scales, like in days, weeks, months or years. Second it gives better options of scales to study extending from a piece of land to several thousand hectares. Third, remote sensing data are made on real time basis which make it more suitable for monitoring current happening phenomenon like wild fires (please refer figure 5). The above given facts make remote sensing a best way to monitor and study deforestation and any activities related to it.

Remote sensing is the only way to get information, when it comes to acquiring data about forests and related activities is inconvenient to collect data from field studies, due to political, topographical, access and similar problems.

Further remote sensing is highly evolving with time. Very high resolution improvements had been made in recent years. In addition to that the quality, quantities and ease of getting remotely sensed data is becoming easier than any time before with the fast advancing technological developments [3]. Which makes

is more reliable and dependable source of data for any kind of studies deforestation.

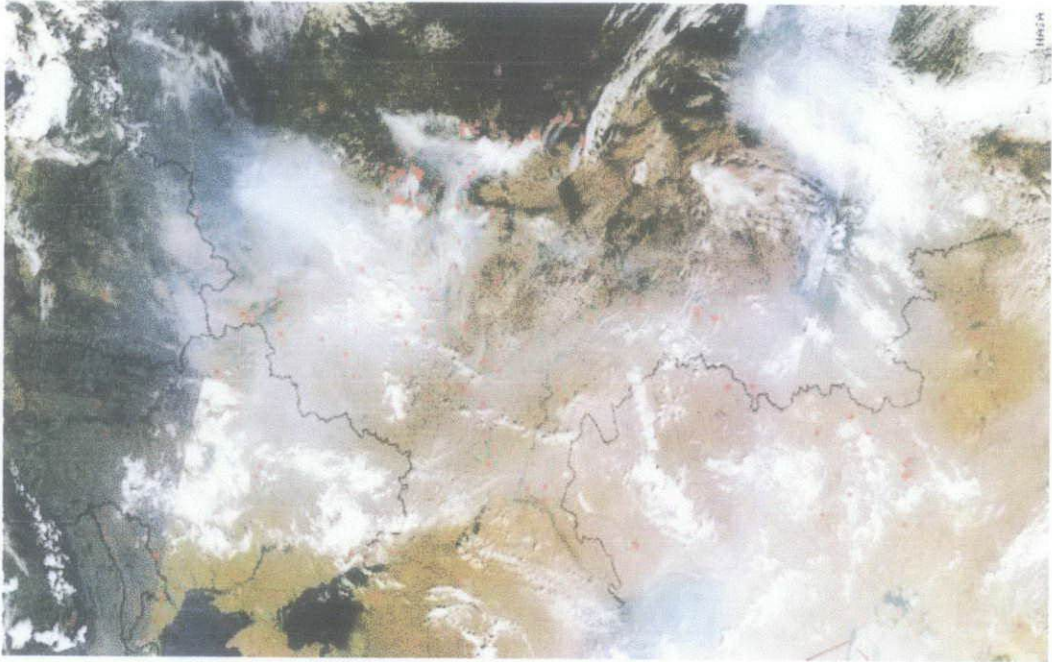


Figure 5 : Russia wildfire, 2010 (Source CNN news [10])

With current advanced technologies high resolution images of any part of the world can be acquired using satellite imaging. Further the images can be taken at any given time and are obtainable with a very high degree of precision. Therefore remote sensing using satellite imaging gives a best way to monitor and control forests and deforestation rates. Hence there are many researches and studies conducted all over the world which are assessment of deforestation based on satellite imaging and remote sensing [1].

This study is also based on satellite imaging to study and implement various algorithms for deforestation analysis. The fast evolution of satellite imaging makes it ideal for the study of forest monitoring and control. Satellite images makes acquiring data of tropical and subtropical regions where information collection from field or ground is quite challenging even impossible for some places.

2.2 Deforestation in relation to human population

Population expansion and general land scarcity caused the rate of deforestation to be at a very high rate through the history of human being. During ancient times forests were easily recovering from natural disasters and degradation coming from anthropological activities. However the population expansion and larger consumptions and dependability on forests and natural resources inhibited forests from recovering naturally. And because of that our earth is facing great dangers of water, soil and environmental pollution problems. Further the plant and animal lives are also experiencing extinction degradation and behavioral changes. And the above all facts faced great concern on sustainability and survival of ecosystems and human life as well.

Based on study conducted by, Institute of Industrial Science, University of Tokyo, Japan, It has been found that population expansion is the main reason which resulted in large scale deforestations. And the study developed a model which predicts the global deforestation rates and forest covers for the future years ahead. The study analyzes human population in relation to forest losses [9]

Further this study showed that if deforestation continues in the current rate, tropical Africa, Saharan Africa and Central America will be leading regions of deforestation by the year 2050. Tropical Africa region will loss 43.67% of the forest coverage from the 1990. Whereas Saharan Africa and Central America will loss 36.87% and 27.87% respectively of the forest cover in 2050. Table 1, in the next page, shows the predictions for deforestation in the year 2050 in terms of statistics and Figure 6 show a map of the predicted deforestation from 1990 to 2050. [9]

The study further showed that if deforestation continued at current rate by the year 2050, 10.54% of world forest cover from 1990 will be lost. This makes it clear that deforestation is at alarming stage and affecting each and every region of the world either directly or indirectly.

Table 1: Deforestation prediction by the year 2050 [9]

Part of the word	Forested area in 1990 (%)	Forecasted forested area in (%)		Deforested area since 1990 (%)	
		2025	2050	2025	2050
Africa (Tropical)	36.94	24.65	20.81	33.27	43.67
Africa (Saharan)	13.52	9.52	8.54	29.62	36.87
Asia (Tropical)	34.81	28.74	26.67	17.44	23.39
Europe	36.78	36.68	36.68	0.26	0.26
Central America	31.58	25.11	22.78	20.50	27.87
Latin America (Tropical)	61.24	53.88	50.04	12.03	18.29
World	33.20	30.5	29.7	8.13	10.54

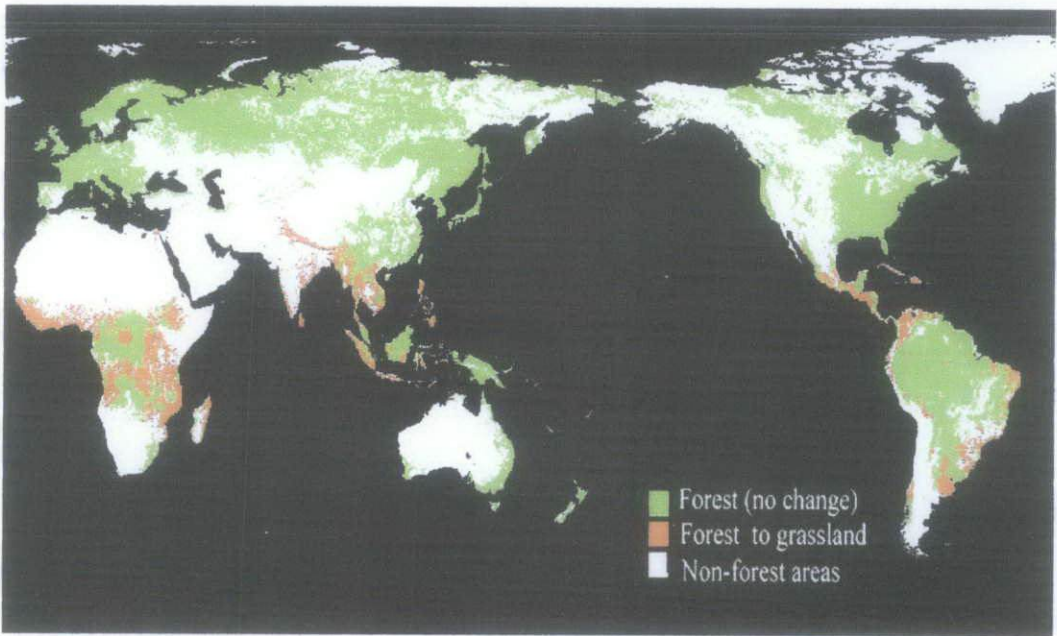


Figure 6: Forest coverage prediction 1990 – 2050 [9]

FAO of UN study showed that there are different agents responsible for deforestation in different parts of the world [3]. Table 2 given below showed the agents and their responsible place of deforestation.

Table 2: Agents of deforestation and their responsible region [3]

Region / part of the world	Deforestation agents
Africa	<ul style="list-style-type: none"> ✓ Nomads and pastorials ✓ Loggers ✓ Mechanized farmers ✓ Shifting cultivation farmers ✓ Wars and consequences
Asia-Oceania	<ul style="list-style-type: none"> ✓ Paper and pulp industries ✓ shifting cultivation farmers ✓ City infrastructure expansions ✓ Loggers ✓ Mechanized farmers
Caribbean & Latin America	<ul style="list-style-type: none"> ✓ Mechanized farmers ✓ Loggers ✓ Shifting cultivation farmers ✓ Nomads and pastorials ✓ City expansions

Forest crisis have provoked and initiated many nations, regional and international preservative initiatives for the control and monitoring of deforestation rates. However all these initiatives didn’t advance and hit their targets because of the fact that most countries didn’t work together with these initiatives and because the initiatives have different strategies, rules and obligations. Further most of these initiatives focus only on the direct causes of deforestations and ignored underlying causes of deforestations, which highly contributed to their slow progress or failure.

In some regions of the world governments made careless decisions which encouraged short-term profit making strategies over long term sustainable growth at the cost of deforestation and unsustainable developments. Further raw material exploration, mechanized farming expansion, countryside exploration by urban

riches, impacts of military and wars, expansion of wood and timber industries and climate change inhibited forestations and became roots factors of deforestation [3]. The following figure gives the main causes of deforestations, both direct causes and underlying causes.

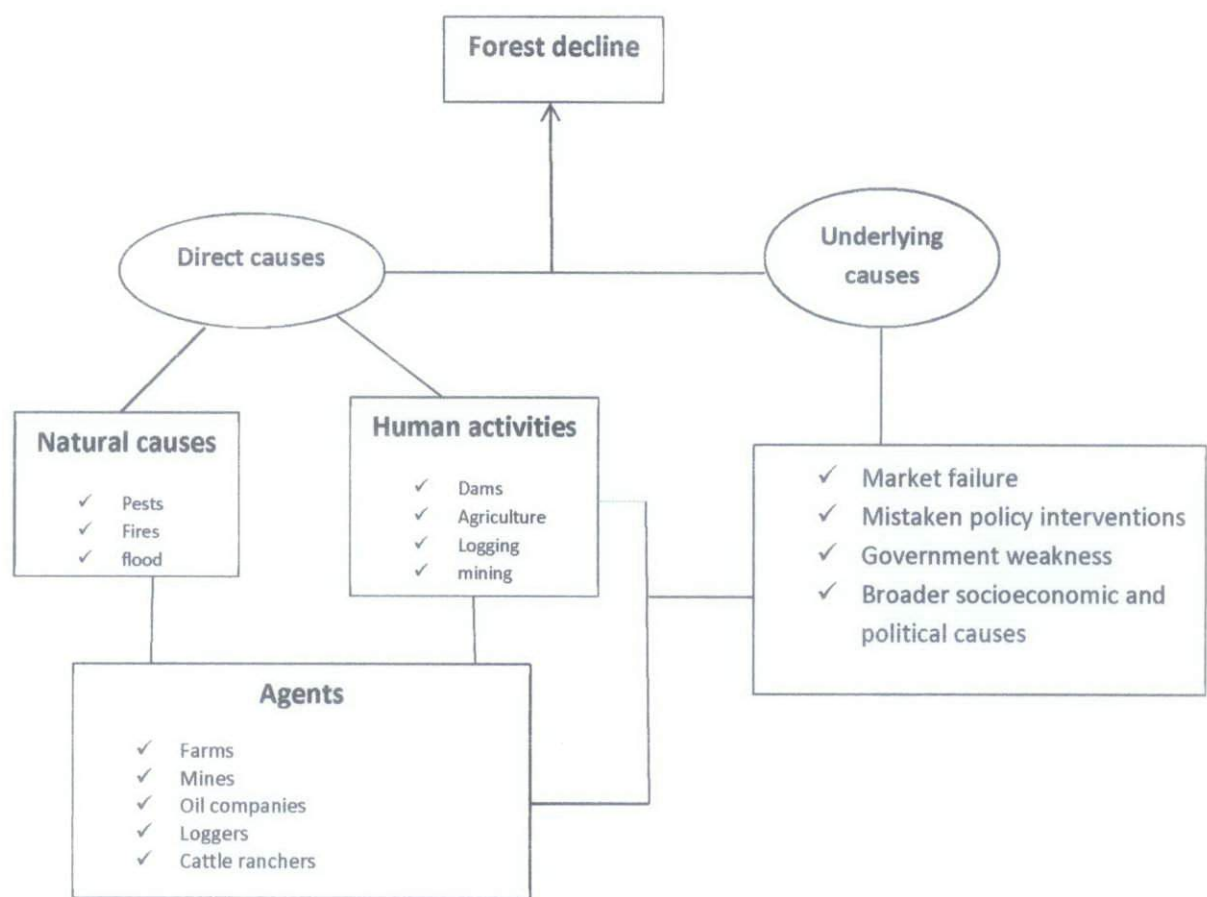


Figure 7 : Causes of deforestations [3]

2.3 Color spaces

2.3.1 L*a*b* color space

*CIE L*a*b** (CIELAB) color space was developed by the International Commission on Illumination. It is the most complete color model which is device independent and used to represent all colors which are visible to human eye.

Color independence of $L^*a^*b^*$ make it ideal to be used as a model in many applications. Further this characteristic makes it easily be observable by human eyes and techniques used to segment and cluster images in to regions. L^* stands for the luminance of color which is also named black, the a^* channel is the pixel position between red and green channels also called green and the b^* channel is the location between the red and blue which is also called blue.

In $L^*a^*b^*$ color system, the L^* channel is the most extremely useful channel containing much of the edge information. Changing the L^* channel will highly affect the original data compared to changing the a^* and b^* channels. The $L^*a^*b^*$ color space is a three dimensional model and can be represented as horizontal slices by assigning the vertical axis to the L^* channel. [18]

2.3.2 HSV and HSI color spaces

HSI (Hue Saturation and Intensity) and HSV (Hue saturation and Value) color spaces are the cylindrical-coordinate representations of points in an RGB (red green blue) color model. Since their introduction in the early 1970's, they are being widely used in digital image processing. Some of their application includes; color picking systems, image editing and color transformation software's and also in computer vision and image processing tools and applications [24].

HSV stands for *hue*, *saturation*, and *value*, and is also often called HSB (*B* for *brightness*). HSI is abbreviation for *hue*, *saturation*, and *intensity*. However, these definitions for abbreviations are not standard and similar everywhere. Hue is the angle from the central vertical vertex axis and saturation is the distance from this central vertical axis, and distance along the axis is value. Although the hue definition is same for both HIS and HSV their corresponding saturation definition is different.

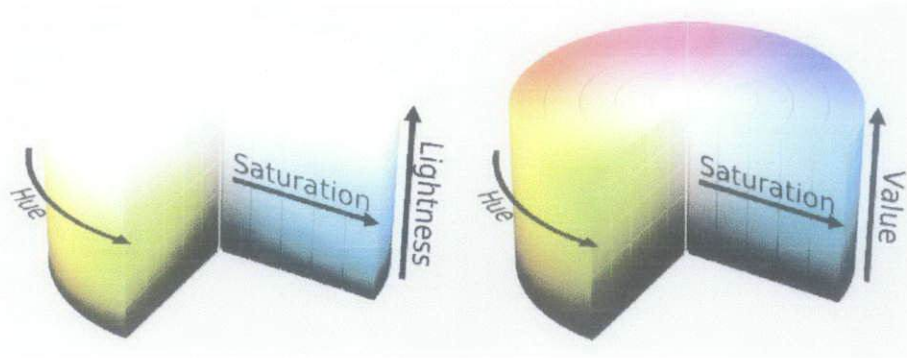


Figure 8: HSI and HSV color spaces

This project is aimed at studying and implementing different algorithms of deforestation analysis using remote sensing. This would have ability to perfectly analyze deforestation rate and also address some of the drawbacks of the current deforestation analysis methods.

CHAPTER 3

METHODOLOGY

3.1 Data Acquisitions

A data acquisition was the first and the most challenging step of this project. It was prime interest to get a similar place or location satellite images taken in different time scales; which can be months, years or decades apart. The purpose of data acquisition is to study and implement the different deforestation analysis algorithms and compare their performances. And also gives clues for what is going on in the world and whether if there is deforestation or not.

It was able to find three images taken from Rodonia, Brazil from U.S. Geological survey, NASA images and few satellite images for Amazon Brazil from NASA IMAGES. The images of Rodonia, Brazil (Lat -10.272756^0 Lon -63.162257^0) were taken in 1975, in 1989 and in 2001. Which are really useful for this project, (Please refer to the image given in Appendix A).

3.2 Feature selection

Once after the satellite images were acquired the next stage was feature selection, which is looking for the channel which contains much of the edge information. To do so the original RGB image was transformed to $L^*a^*b^*$, HSV and HSI color spaces and each channels were studied and passed through different deforestation analysis algorithms. (Please note that the results of this stage will be discussed in depth in the Result and discussion section, Chapter 4).

3.3 Satellite (Digital) image processing

The ease of accessing and getting satellite remote sensing data makes deforestation monitoring and controlling possible. Therefore deforestation analysis using satellite sensed data studies formulated different models which predicted and analyzed for the forest which existed before and going to exist in the future. Satellite images make deforestation pattern studies, rate of deforestation studies and main causes of deforestation studies easier, timely and cheaper. [11]

Continuous advancements and improvements in image analysis and pattern recognition contributed to analyzing and studying deforestation patterns and rates. Recent image segmentation, pattern recognitions and region clustering play important role in deforestation analysis using remote sensing [12]

3.3.1 Image Segmentation, Otsu method

Image segmentation is separating or dividing of images into different clusters or regions based on common properties and/or differences between other regions properties. One of the many and simple property that can be applied to separate images in to regions is pixels intensity. So we normally can segment images into different regions through thresholding or separating the pixel levels into different scales. These different thresholding scales create different regions corresponding to the pixel intensity values. A simple example can be thresholding a gray scale image pixels in to two regions, that is transforms the gray scale image in to binary image, which will consist of only two regions that is either dark or white.

If $G(x, y)$ is a thresholded version of $f(x, y)$ at some global threshold Th ,

$$G(x, y) = \begin{cases} 1 & \text{if } f(x, y) \geq Th \\ 0 & \text{otherwise} \end{cases}$$

OTSU (a segmentation method named after Nobuyuki Otsu) **segmentation method** uses a method which transforms a gray scale image in to a binary image with two pixels values of either black (0) or white (1) pixels. OTSU's segmentation is a histogram shape-based image segmentation which sets the thresholding value automatically. The Otsu algorithm always takes an image and assumes that it has only two classes of pixels and then calculates the best thresholding values to perfectly segment these two classes so that the intra-variance difference will be kept very small. Otsu has reformulated this problem so that it can be computed efficiently with histograms. (Please note that this method is applied in this project and the result will be discussed in depth in the Result and discussion section, Chapter 4).

3.3.2 Image clustering

Content based image clustering; CBIR has been one of the main interests in computer vision and image processing recently. The main interest of clustering an image is to group or classify objects in to different classes which have similar properties. These classifying of images in to groups help us study different characteristics of the image like pattern, flow, changes and similarity of events or phenomenon. Further clustering of images gives clusters or regions with detailed and concise information and content of the images which ease the task of studying this regions or clusters. So an image clustering is a very systematic and description of an image contents [21].

FCM (Fuzzy C-mean) is the most one of the most common form of image clustering and it is based on the principle of fuzzy classification. Fuzzy c-mean clustering was developed by Bezdek in 1981. It is one of the most used techniques in image clustering and segmentation, pattern recognitions and image processing [22]. In Fuzzy c-mean clustering, pixels with identical properties will be grouped in to same categories or clusters. Members of a particular cluster or groups have common or identical properties where as they have clear or observable differences with other cluster or group members. In fuzzy c-mean clustering this similarity or

dissimilarity of particular group members are measured by computing the distance of pixels from threshold values.

The fuzzy c-mean clustering algorithm is based on iterative minimization of difference in the cluster centers. Fcm starts computing segmentation or clustering of images first by guessing specific values for threshold values. These threshold values are pixels value limits, which are used to divide and group the image pixels into different groups and regions. However since these initial values for the cluster centers are guess, most of the time they are incorrect. Therefore the fcm algorithm continuously upgrades and moves this cluster centers iteratively to the ideal or rite position. So by continuous moving of the initial cluster centers, it precisely clusters the image in to different regions and improves the accuracy of the membership grades of each groups [23].

Fuzzy c-mean clustering, after the initial cluster guess center, continuously moves and updates the cluster centers towards the exact logical pixels values. And we can set and manipulate the iteration number or membership grade limit qualities, or in other terms, maximum change of pixel changes by specifying stopping threshold criteria's [22].

The input images for the fuzzy c-mean clustering were gray scale images and the cluster centers were computed automatically by the function itself. Once the cluster center was found and fixed the next stage was setting the rules for fuzzification. The, if - then rules are given below; (assuming the three cluster values are Cluster-1, Cluster-2 and Cluster-3);

If pixel (i,j) is less than cluster-1 center make it black (0)

If pixel (i,j) is greater than cluster-3 center make it white (1)

Else make pixel (i,j) in between black and white (0.5)

After the rules were executed in the gray scale image the output will be still gray scale image with three clusters or objects. Therefore the results were transformed into a binary image using Matlab built in function. (Please note that this method

is applied in this project and the result will be discussed in depth in the Result and discussion section, Chapter 4).

3.4 Tools and equipment used

The tool and equipment used in this project is MATLAB R2009b which is a very powerful tool for image processing's. In addition adobe Photoshop was used to make the manual/pen segmentation for the ground truth or reference data.



Figure 9: Tools used

CHAPTER 4

RESULTS AND DISCUSSION

4.1 Color space transformations and feature selections

L*a*b*, HSV and HSI color transformations were carried on the original images so that the result show which channel contained much of the edge information, be easily observable, and analyzed by human eye. The L*a*b* transformation was carried on the original image using a build in function of MATLAB. And HSV transformation was also carried using a Matlab built in function. Whereas for the HSI transformation a code was generated and used. (The code used to carry the HSI transformation is given in Appendix B)

Once the result of the L*a*b*, HSI and HSV were obtained, the next task was applying the Otsu algorithm of segmentation and fuzzy c-mean clustering on the three channels of the three results. And then further analyze the result and find out which channel gives the better result for further analysis.

The three color transformations and segmentations of each channels were carried in one selected image of Amazonian Brazil and based on the results obtained, it was found that L* channel of (L*a*b*) and I channel of the (HSI) and the V channel of the (HSV) color space contained much of the edge information's. (Please refer to the MATLAB code used to generate the result provided in Appendix C at the back of this report).

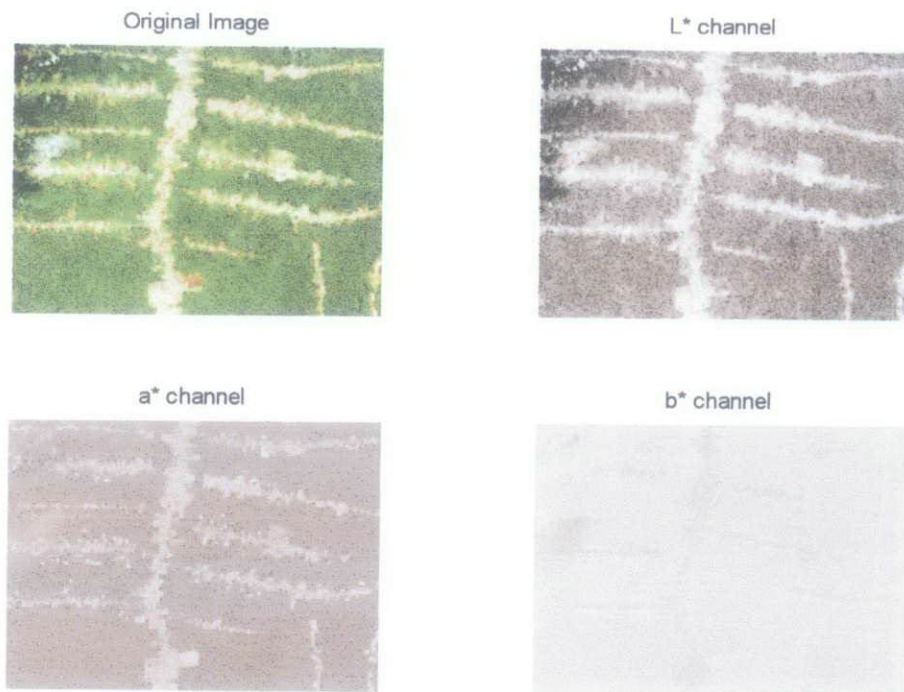


Figure 10: $L^*a^*b^*$ color space transformation

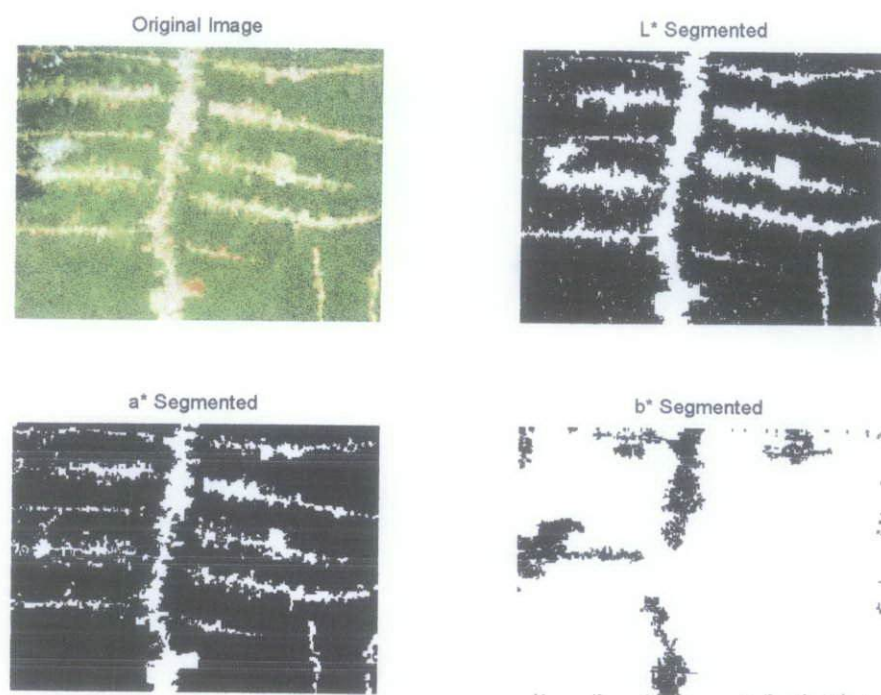


Figure 11: $L^*a^*b^*$ color space OTSU segmentation

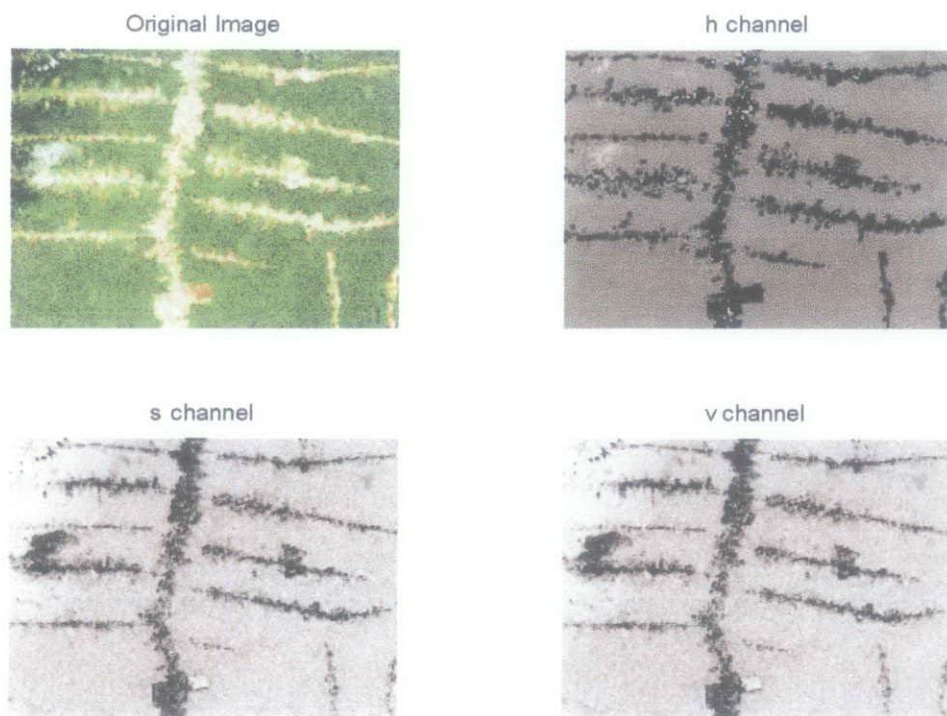


Figure 12: HSV color space transformation

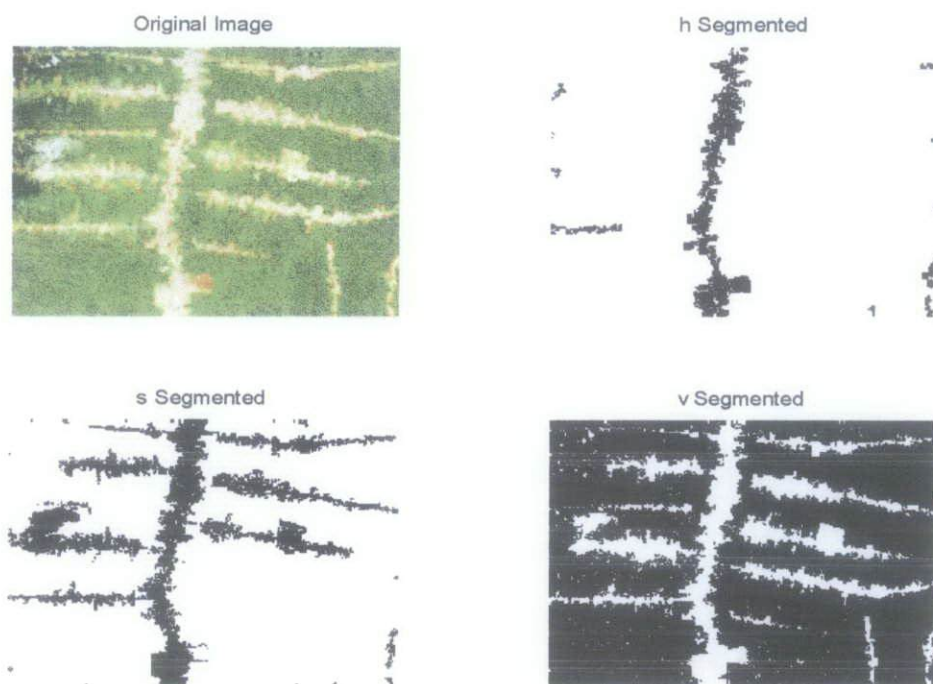


Figure 13 : HSV color space OTSU segmentation

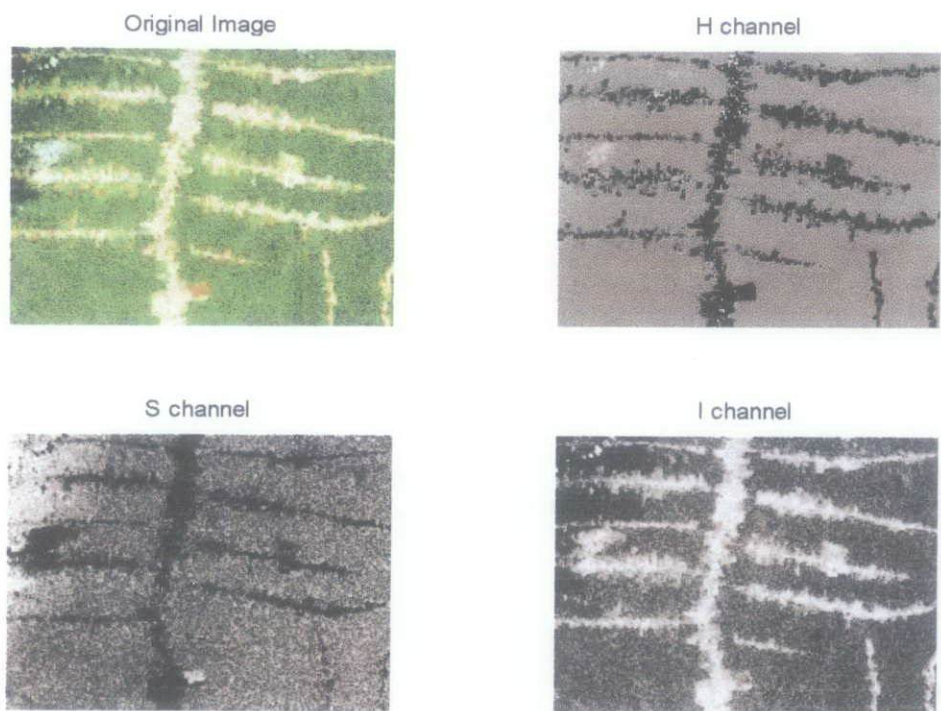


Figure 14: HSI color space transformation

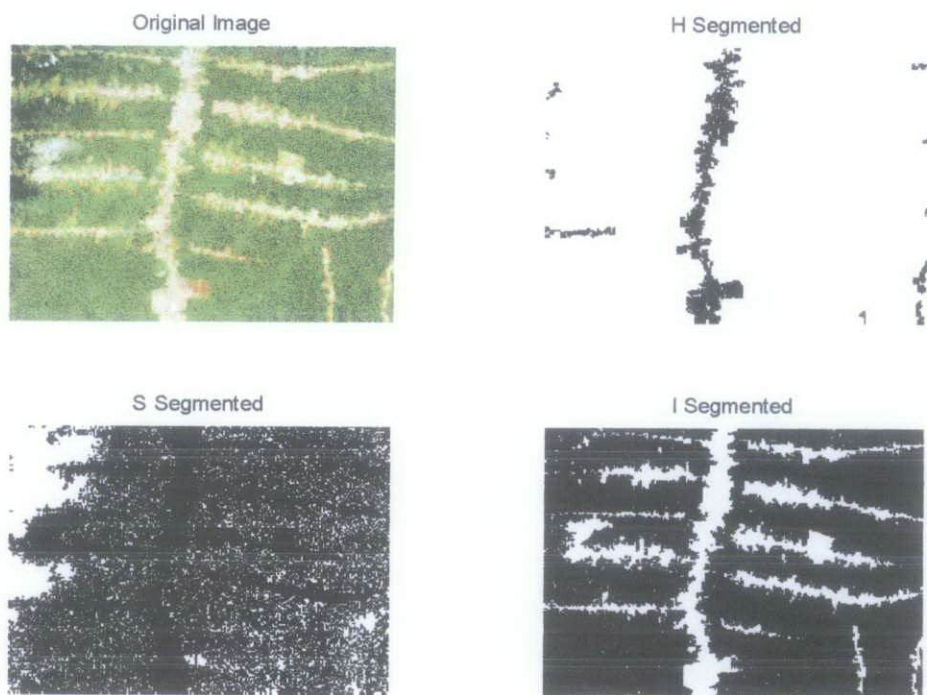


Figure 15: HSI color space OTSU segmentation

From (Figure 10 and 11) it is clear that a better result of segmentation was obtained from the L^* channel segmentation of the $L^*a^*b^*$ color space. The L^* channel segmented image which is the top right image in Figure 11 is the segmented image of the original image based on Otsu algorithm, region of interest (ROI). And hence the L^* channel contains much of the edge information it is chosen for further study.

Further from figures 12 and 13 it is found that the 'I' channel of the HSI color space contained much of the edge information and gives superior result in the OTSU region of interest segmentation. In addition from figures 14 and 15, it is found that the 'V' channel of the HSV color space contain much of the edge information and give better result from the other two channels in the OTSU segmentation.

In the segmented images the black part shows the areas where there is no change that is no deforestation, whereas the white part of the image shows the place where there is change or deforestation. Once the best channels from each color space were selected the next task was to implement and analyze different algorithms for deforestation analysis and compare the result, which will be detailed in the next section.

4.2 Deforestation analysis algorithms implementation and analysis

In this project two deforestation algorithms were implemented studied and then analyzed and compared with the ground truth data. The two methods implemented are the OTSU segmentation and fuzzy c-mean clustering. For this specific part of the project images from Rodonia, Brazil taken in year 1975, 1989 and 2001 are used.

4.2.1 Ground truth data

As reference to compare and analyze the deforestation analysis algorithms performances a ground truth data was needed. And for that a ground truth data was computed by Pen or manual segmentation in Adobe Photoshop. This process was quite lengthy and took hours to be completed. All the three ground truth images are given below;



Figure 16 : Ground truth data for 1975

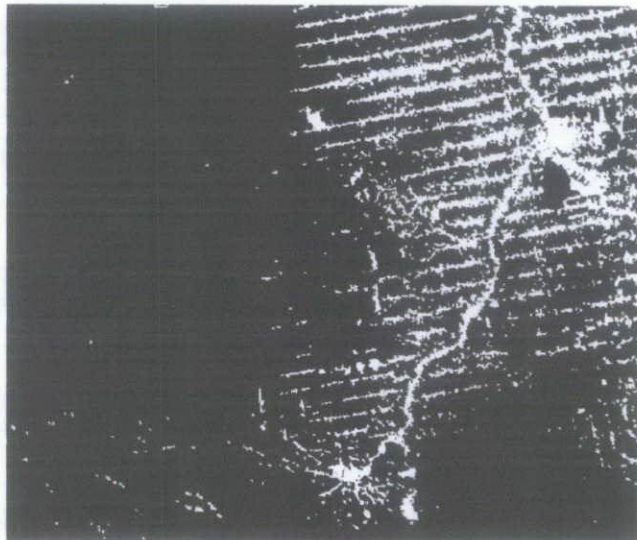


Figure 17: Ground truth data for 1989

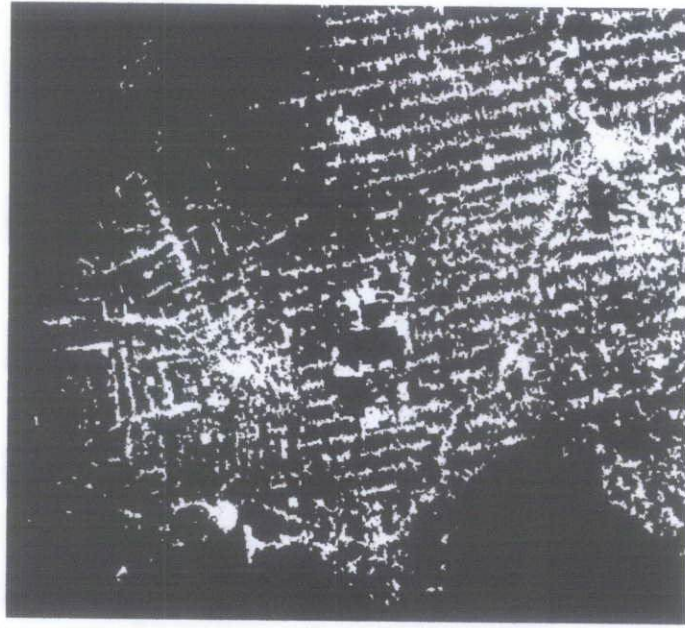


Figure 18: Ground truth data for 2001

4.2.2 OTSU segmentation and Fuzzy c-means clustering

Images of Rodonia, Amazon basin from U.S. Geological survey, NASA images, which were taken in year's 1975, 1989 and 2001, were used and subjected to the same segmentation and clustering algorithms and obtained different results. The OTSU segmentation and Fuzzy c- mean clustering were applied to the selected features and channels chosen based on more edge information contents. Therefore L^* channel from $L^*a^*b^*$, V channel from HSV and I channel from HSI were used to compare and analyze the algorithms performance.

First fuzzy c-mean clustering codes were implemented on the three images of Rodonia, Brazil and then the clustered image were changed to binary image using Matlab built in function in order to compare the results with the OTSU segmentation and restrict the region of interest only to the deforested areas. Then after the Fuzzy c-mean clustering, all the selected channels were again subjected to the OTSU segmentation. Then the results from both methods were compared

with the ground truth data. (Please note that all the codes used to implement the OTSU segmentation is given in appendix D and the Fuzzy c-mean in appendix E)

4.3 Accuracy assessment

The results of the segmentation and clustering were assessed and compared with the ground truth data. For this task correlation and root mean square error were computed. For correlation computation a Matlab build in function is used and to implement the correlation of the processed image with the reference image first both data were needed to be reshaped in to a single column matrix and that was also carried out by Matlab build in function. For the root mean square error, since the processed and reference images are in binary form (either 0 or 1) the root mean square error was computed directly on the reshaped images.

Correlation is a statistical technique that shows the degree of relationship or similarity between any two given variables. Correlation is used to determine whether two variables are related or not, and if they are related it tells us how strong is the relation between the variables. Therefore correlation results in a single number which can vary from 0 to 1 showing the degree of relation. Correlation result can range from 0 to 1. 1 shows that the variables are identical and 0 tells that the two variables are not similar or related.

The root mean square error (RMSE) is a measure accuracy assessment which gives us the difference of the original data modeled or being estimated and the result of the predicted or estimated model. Root mean square is a perfect measure for accuracy and a very small value of RMSE is ideal for perfect estimation or approximation of a data or variable or better result.

Correlation and root mean square analysis were computed to find out which channel from the L^* of $L^*a^*b^*$, V of HSV, and I of HSI color space give superior result and resembles the Ground truth data. Please take note that the higher the

correlation (closer to 1) is the better and the lower RMSE (root mean square error) closer to zero is the better. (Please note that all the codes used are given in Appendix D and E), and the results are given in the following tables below;

Table 3 : Fuzzy c-mean clustering result

Image	FCM			
	Channel	RMSE	Correlation	Best
1975	L (L*a*b*)	0.002338504660713	0.692304364392193	L*
	I (HIS)	0.002603317906264	0.643651454172925	
	V (hSV)	0.002652206505443	0.635072529709369	
1989	L (L*a*b*)	0.030372420323929	0.840437802029339	L*
	I (HIS)	0.039323733019854	0.790056668128420	
	V (hSV)	0.034797054597701	0.815646069194413	
2001	L (L*a*b*)	0.033949820788530	0.876394957084050	I
	I (HIS)	0.029841269841270	0.890571656134183	
	V (hSV)	0.044165898617512	0.833409983436552	
Overall				L*

Table 4: Otsu segmentation result

Image	OTSU			
	Channel	RMSE	Correlation	Best
1975	L (L*a*b*)	0.003055537448667	0.559334400600003	L*
	I (HIS)	0.003198129196271	0.529991402025284	
	V (hSV)	0.003165536796819	0.536839043103919	
1989	L (L*a*b*)	0.022421140282132	0.884549908627984	L*
	I (HIS)	0.023123204022989	0.881192441998460	
	V (hSV)	0.026494742685475	0.862290862921132	
2001	L (L*a*b*)	0.135885304659498	0.677868742421976	V
	I (HIS)	0.142013312852023	0.668171288758066	
	V (hSV)	0.105065028161802	0.731108743480470	
Overall				L*

Table 3 and 4 shows that the L^* channel of $L^*a^*b^*$ color space gives better results, that is higher correlation and minimum RMSE, compared with V of HSV and I of HIS on both OTSU and fuzzy c-mean based segmentations. The following bar graph comparisons proves the above mentioned point. (Please note that Appendix H gives all the segmented images)

FCM method

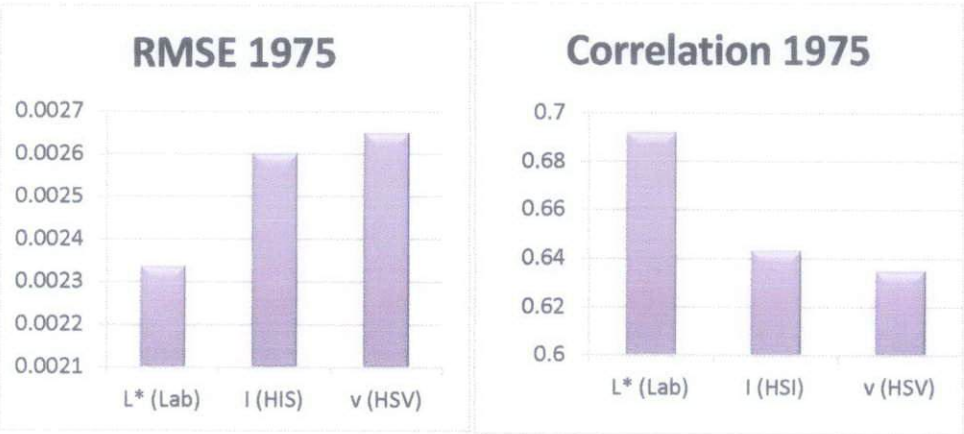


Figure 19: 1975 RMSE and correlation FCM

Figure 19 shows that the L^* channel clustering and then transformation to binary image gives better correlation and minimum RMSE compared to I and V channel equivalents.

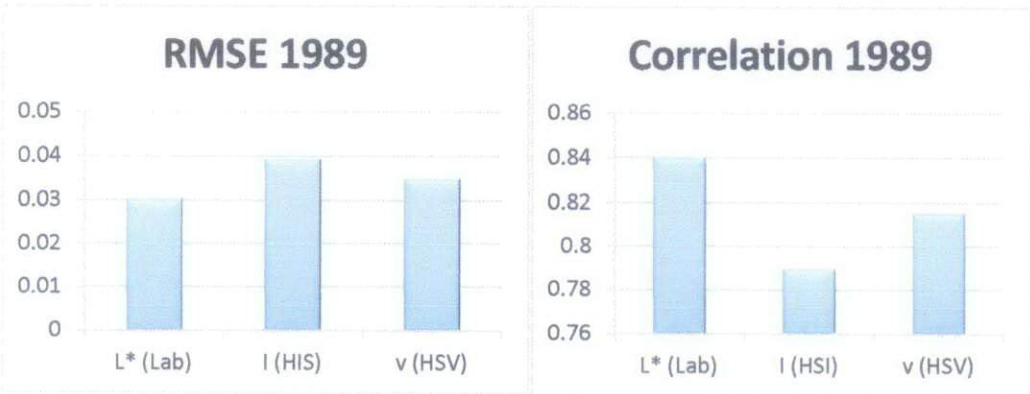


Figure 20: 1989 RMSE and correlation FCM

Once again in figure 20 shows that the L* channel clustering and then transformation to binary image gives better correlation and minimum RMSE compared to I and V channel results.

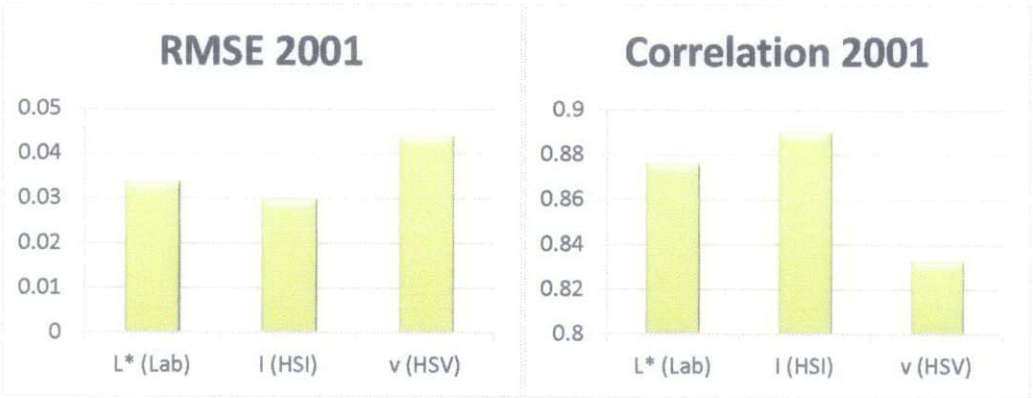


Figure 21: 2001 RMSE and correlation FCM

Here figure 21 shows that the V channel clustering and then transformation to binary image gives better correlation and minimum RMSE compared to L* and I channel results. But here we can see that L* channel result is not much apart from the V channel result. So overall for the fcm clustering the L* channel gives the best result compared to V and I counterparts.

OTSU Method

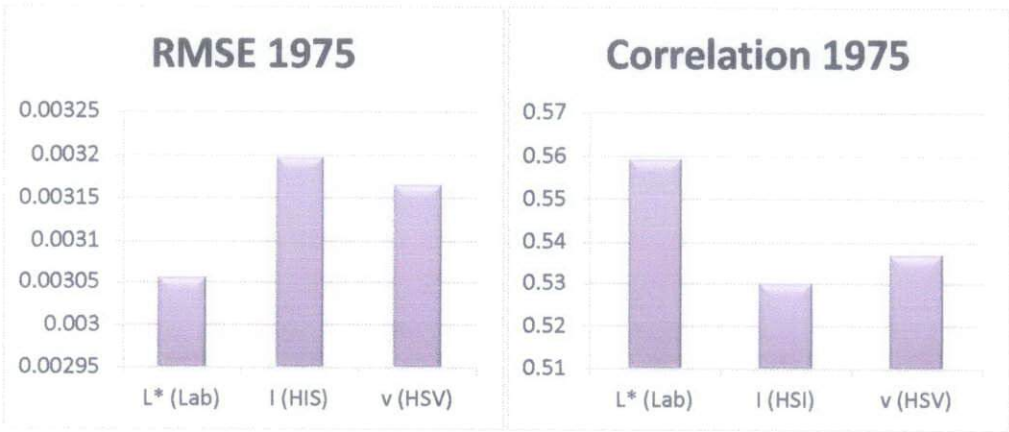


Figure 22: 1975 RMSE and correlation OTSU

For the OTSU segmentation of the 1975 Rodonia, Brazil image the L* channel of the L*a*b* color space gives the best result that is lower RMSE and higher correlation compared to I and V channels.

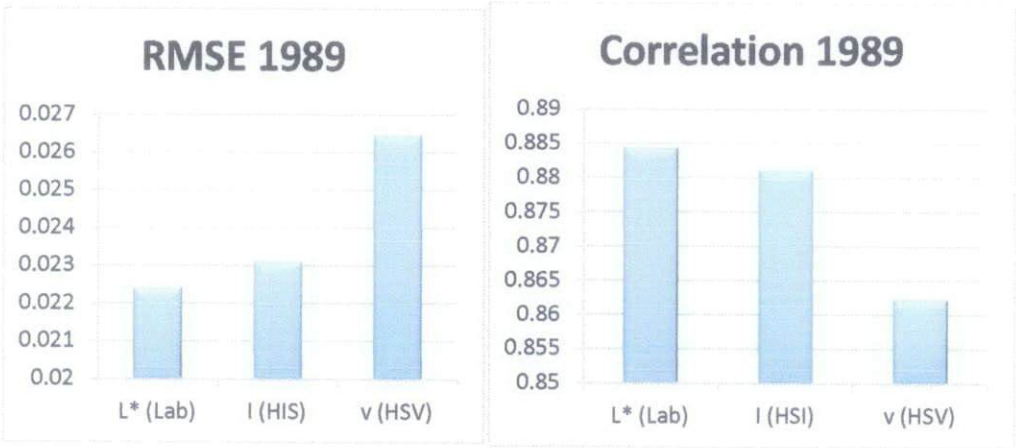


Figure 23: 1989 RMSE and correlation OTSU

Once again for the 1989 Rodonia, Brazil image OTSU segmentation of the L* channel of the L*a*b* and I channel of HIS color spaces give approximately equal results that is lower RMSE and higher correlation compared to the V channel of the HSV result. However still the L* channel has better result compared to I channel result. Hence once again the L* channel is better than the other two.

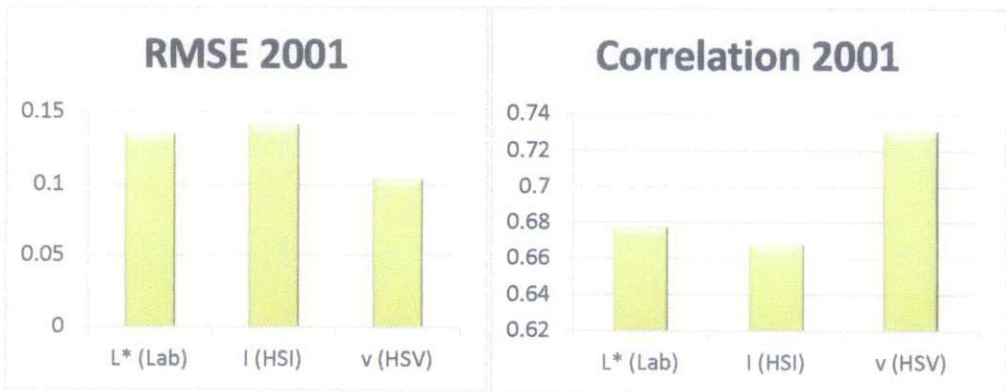


Figure 24: 2001 RMSE and correlation OTSU

Here for the 2001 OTSU segmentation image the I channel of HSI gives better result compared to the L* and V channel results. However it is observed that the L* channel result is pretty close to the HSI channel result.

Overall for the OTSU based segmentation the L* channel is better compared to the other two. Therefore combining the results obtained by the fuzzy c-mean clustering and OTSU segmentation it is concluded that the L* channel of L*a*b* color space gives the best result and it will be used for further analysis.

4.4 Comparison between Fuzzy c-mean clustering and OTSU segmentation

Once that the L* channel found to contain much of the edge information and gives better result compared to I and V channels. The next task was to compare and decide which algorithm gives the better result for the deforestation analysis. Here also the reference is the ground truth data acquired from the manual segmentation in the adobe Photoshop.

The results obtained from the fcm and Otsu methods are summarized and the corresponding best results for each image were taken and analyzed below. The following table and graph shows the comparisons between the two methods.

Table 5: fcm and Otsu comparison

Image	Method	RMSE	Correlation
1975	FCM	0.002338504660713	0.692304364392193
	OTSU	0.003055537448667	0.559334400600003
1989	FCM	0.030372420323929	0.840437802029339
	OTSU	0.022421140282132	0.884549908627984
2001	FCM	0.029841269841270	0.890571656134183
	OTSU	0.105065028161802	0.731108743480470

The result in the above table can better be showed and analyzed using the following bar graphs shown below.

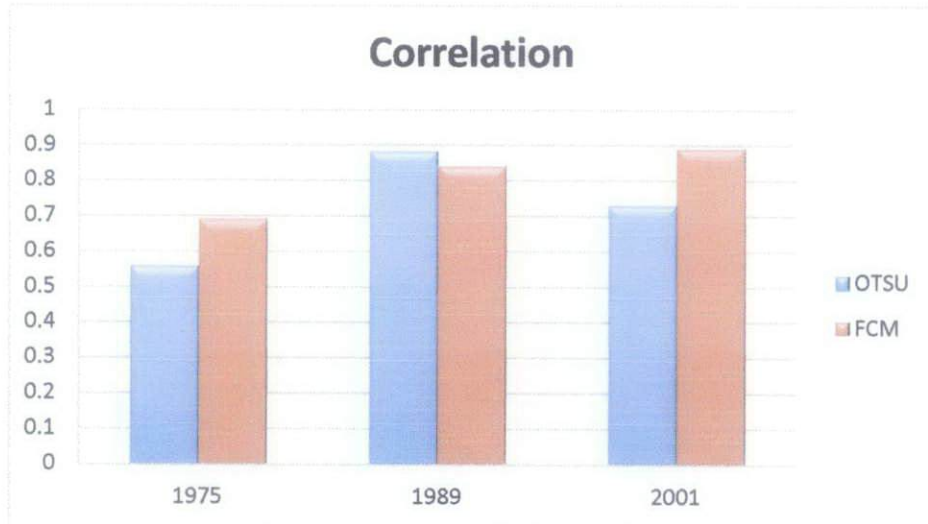


Figure 25: Correlation comparison of fcm and Otsu

Figure 25 shows that Fuzzy c-mean clustering gives better correlation to the ground truth data compared to the Otsu segmentation. The Otsu segmentation exhibits series problem when the deforestation rate is very high. This is observed in the 2001 image segmentation.

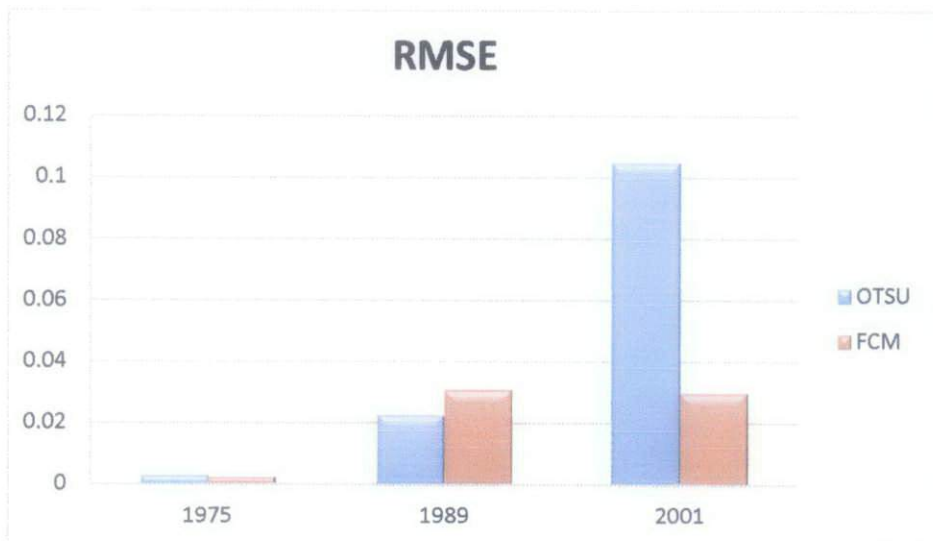


Figure 26: RMSE comparison of fcm and Otsu

Figure 26 proves that the fuzzy c-mean clustering gives minimized root mean square error compared to OTSU segmentation. Which overall makes the Fuzzy c-mean clustering better than OTSU segmentation.

4.5 Application of Fuzzy C-mean clustering in selected images

Once the fuzzy c-means clustering was found to be the best segmentation for this project, it was applied to certain selected images and the correlation and RMSE of the segmented images were computed with the manual segmented images correspondingly.

All the images used are taken from NASA Images and here is a table summarizing the accuracy assessment of the Fuzzy C-mean cluttering versus the ground truth data. Table 6 proves how Fuzzy C-mean cluttering gives results which are very close to the manually segmented ones. (Appendix F gives the original images and the segmented ones).

Table 6: fcm clustering results

Image	Correlation	RMSE
Rondonia, Brazil 1975	0.692304364392193	0.002338504660713
Rondonia, Brazil 1989	0.840437802029339	0.030372420323929
Rondonia, Brazil 2001	0.834394702888729	0.055864823348694
Amazon, Brazil 2003	0.812590866051832	0.054560185185185
Amazon, Brazil 2004	0.832662996995006	0.059369212962963
Amazon, Brazil 2005	0.822184576210836	0.065978009259259
Amazon, Brazil 2006	0.832842193498467	0.065439814814815
Amazon, Brazil 2008	0.784082370991039	0.091296296296296
Amazon, Brazil 2009	0.843561518608675	0.063373842592593
Amazon, Brazil	0.917434437596618	0.022502310643417
Matogrosso	0.815897702760996	0.031324444444444

4.6 Real case scenario application of the Fuzzy c-mean clustering

The fuzzy c-mean clustering algorithm is next applied to a real case scenario that is deforestation in Rondonia, Brazil. Rondonia is one of the states in Brazil, which

is widely known for its vast amazon rain forest jungle, it is located in the north-western part of Brazil. Rodonia borders with state or Acre the state of Amazonas, Mato Grosso and Bolivia.

Rodonia state is one of the most densely forest covered regions of amazon forests. However a considerable amount of forests have been removed or cleared by anthropogenic activities beginning in the late 1970s. Rodonia is now well known wood exporter and much of the forest has been changed to urban settlement area [20].

The area used for this study in this project is located at -10.272756^0 latitude and -63.162257^0 longitudes. The images for the studies are taken from U.S. geological survey, NASA Images. The images are taken in three different years, 1975, 1989 and 2001.

Once the Fuzzy C-mean clustering implemented on the three images' of Rodonia Brazil forest, the next task was to compute how the deforestation rate is affecting the place and calculate and analyze the total area affected in each three images. This in turn could help in forecasting what will be the forest coverage after some years if the deforestation continues in the current rate.

The area affected in each segmented images is calculated by a MATLAB build in function. The build in function computes the area of objects in a binary image. The original versus the segmented images and the total deforested areas are given below. (Please refer to the Matlab code given in Appendix G)

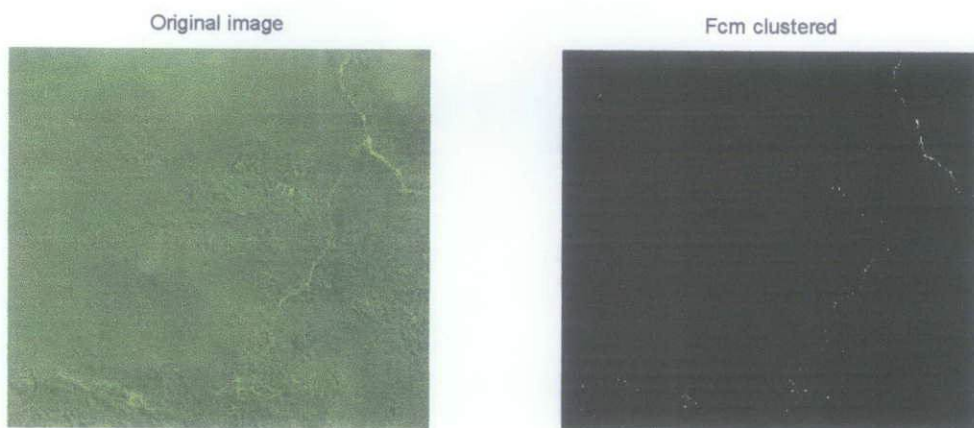


Figure 27: 1975 original versus fcm segmented image

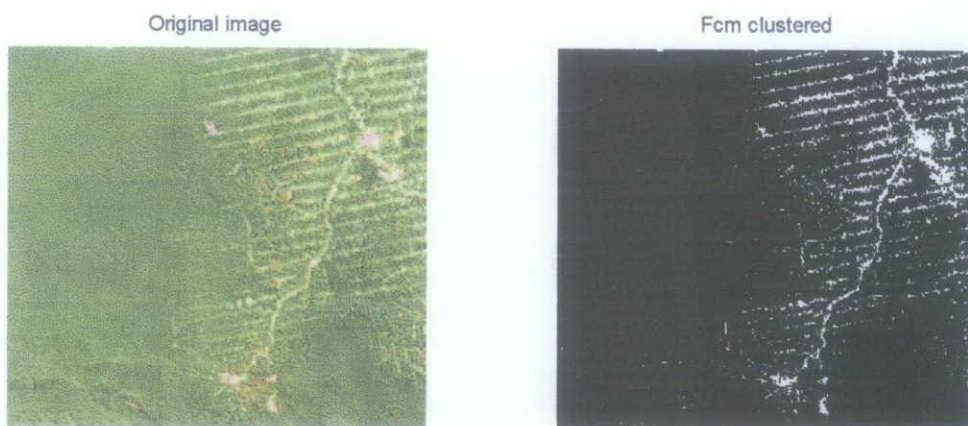


Figure 28: 1989 original versus fcm segmented image

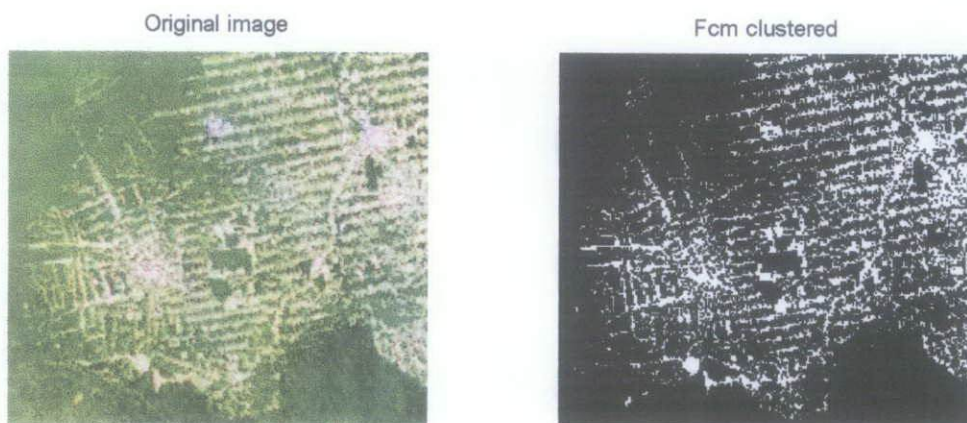


Figure 29: 2001 original versus fcm segmented image

Table 7: Percentage of deforested area computed

Image	Deforested area
1975	0.2479568639593%
1989	8.9546801528213%
2001	17.0550435227855%

The result above in Table 7 clearly showed that the deforestation rate is quite high and by the year 2001(in 26 years), 16.812% of the area has undergone change and is completely deforested.

4.6.1 Future deforestation prediction of Rodonia

The segmentation and area computation of the three separate images takes the project in to the position of estimating the deforestation rate for the years ahead. For this stage both Matlab and excel 2010 is used to find line trend / regression. And in both ways same polynomial equation, degree of 2, approximated the line perfectly with regression of 1(100%). This estimation of deforestation is valid only if the deforestation rate continues at the same rate as it is now. Here is the Matlab command line used to generate the equation of the polynomial function

```
>> x = [0; 14; 26];
>> y = [0.247956864; 8.9546801528213; 17.0550435227855];
>> p = polyfit(x,y,2)
p =
    0.0020    0.5933    0.2480
```

$$Y = 0.002 * X^2 + 0.5933 * X + 0.248$$

Where: Y = Deforested area

X = Number of years starting from 1975

This result means that the deforestation area/rate can be computed or forecasted for the future years using the above equation. And based on the above equation the deforestation prediction is given by the following graph as follows;

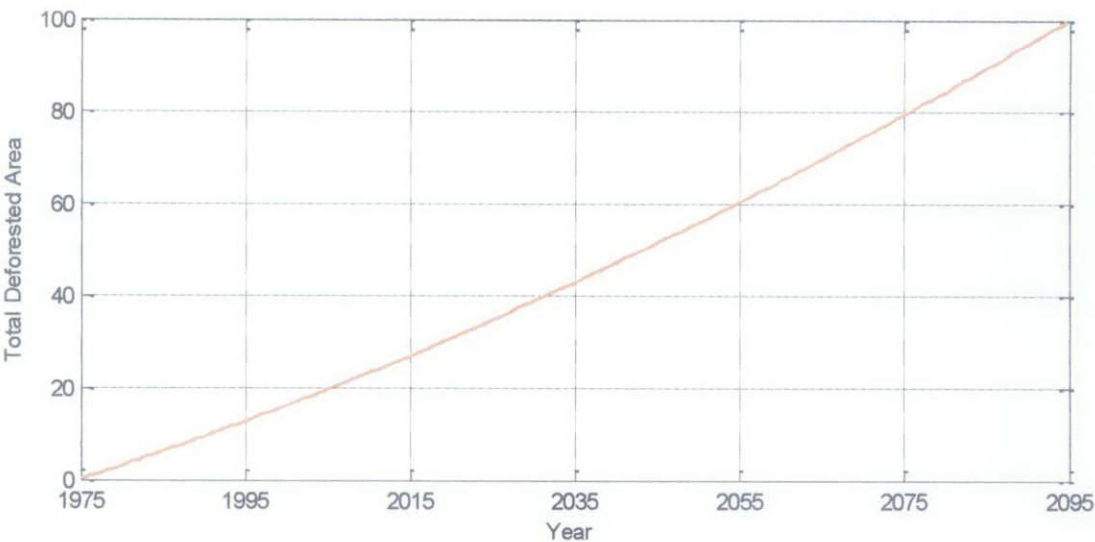


Figure 30: Deforestation prediction for Rodonia, Brazil

Therefore the above graphs shows that if deforestation continues at a current rate in Rodonia, Brazil, by the year 2025 the deforested area will be 34.9130%, by the year 2050 it will be 56% and by the year 2095 all the area will be 100% deforested. This result shows that the deforestation rate in the area is very high and urgent measures should be taken to control it.

CHAPTER 5

CONCLUSION AND RECOMMENDATION

Deforestation is affecting our unique world Earth and plants and animals lives are facing great dangers and consequences. Because of deforestation, plants and animals are being extinct and because of that the species and genetic diversity of living things is getting lower and lower from time to time. Further it is believed that reduction of plant and animal biomass and biodiversity could have unforeseen complications in the future. It is also known that because of deforestation climates and environments are undergoing wide ranging changes affecting all living things including humans which are the main causes of deforestation. Further human beings are subjected to the moral and ethical responsibility of preserving all living things and beauty of earth.

So in view of increasing deforestation and all its negative impacts it is highly necessary to take urgent measures to monitor forests to check and control deforestation rates. It is also necessary to take all essential measures to restore forests so that better forest qualities will be kept and hence meet wide human and non-human needs. All forest management systems and principles should be coordinated and implemented based on the principles of sustainability. Measures taken should be appropriate, socially beneficial and economically viable. The main reason of maintaining forests is the conservation of biodiversity at the genetic, species, and ecosystem levels.

Based on the results obtained in chapter 4, Fuzzy c-mean segmentation applied on L^* channel of $L^*a^*b^*$ color space gives binary image. These binary images comprise only two pixels, black pixels (0) or white pixels (1). And this segmentation results eases the task of deforestation analysis which is calculating

the area of deforestation and/or possibly take the difference of the segmented images of the different years and observe and analyze the difference.

Further Fuzzy c-mean deforestation analysis gives a good result in deforestation analysis and can be used as a structured assessment of deforestation. It can be used to check deforestation and control the rate and hence help fighting the great danger of deforestation world-wide. If this code is implemented it can clearly show not only deforestation rate but also afforestation rate.

REFERENCES

- [1]. Mesgari Saadi, and Ranjbar Abolfazl, 'Analysis and estimation of deforestation using satellite imagery and GIS', Geodesy and Geomatics Dept., Faculty of Civil Engineering, K.N. Toosi University of Technology, 2003
- [2]. Ziyu WANG, Wenxia WEI, Shuhe ZHAO and Yuanhua LUO, 'Detection of Forestland degradation using Landsat TM data in panda's habitat', Sichuan, china , 2004
- [3]. Giri tejaswi, 'Manual on deforestation, degradation, and Fragmentation using remote sensing and GIS', Forestry department, Food and Agriculture organization of the United Nation (FAO), Rome, March 2007
- [4]. Deforestation , retrieved on August 10, 2010, from http://en.wikipedia.org/wiki/Deforestation#Controlling_deforestation
- [5]. A. Thayalan, F.S. Abas, V.C. Koo, 'Automatic change detection of Belum-Temengor forested area using multitemporal SAR images', Faculty of engineering and technology, multimedia university Jalan Ayer Keroh Lama, Bukit Beruang 75450, Melaka, Malaysia, 2009
- [6]. Pavan kumar, Meenu Rani, P.C. Pandey. Arnab Majumdar and M.S. Nathawat, 'Monitoring of deforestation and forest degradation using remote sensing and GIS', 2010
- [7]. C.J. Tucker and J.R.G. Townshend, 'Strategies for monitoring tropical deforestation using satellite data', laboratory for terrestrial physics, NASA/Goddard space flight center, 2000
- [8]. Michael Palace, Michael Keller, Gregory P. Asner, Stephen Hagen and Bobby Braswell, 'Amazon Forest Structure from IKONOS Satellite Data and the Automated Characterization of Forest Canopy Properties', 2008

- [9]. Krishna PAHARI, Shunji MURAI, Yoshifumi YASUOKA, 'Sustainability analysis for human population in relation with global deforestation using remote sensing and GIS', Institute of Industrial Science, University of Tokyo, Japan
- [10]. Satellite images show scope of Russian wildfire, retrieved on August 16, 2010, from
http://edition.cnn.com/2010/WORLD/europe/08/14/russia.wildfires.nasa/index.html?hpt=T1#fbid=LQQb5_ASXK8&wom=true
- [11]. Olimpia arellano-Neri and Robert C. Frohn, 'Image based logistic Regression parameters of deforestation in Rondonia, Brazil', department of Geography, University of Cincinnati, Cincinnati, Ohio, 2001
- [12]. Matteo Sgrenzaroli, Andrea Baraldi, Hugh Eva, gianfranco De Grandi, 'Contextual Clustering for image labeling: An application to degraded forest assesment in Landsat TM images of the brazilian amazon', August 2002.
- [13]. Joao Roberto dos Santos, 'Monitoring land use in Amazonia based on image segmentation and neural networks', INPE-Instituto Nacional de Pesquisas Espaciais, Brazil 1995.
- [14]. Liana O. Anderson, Yosio E. Shimabukuro, Ruth S. Defries, and Douglas Morton, 'Assessment of deforestation in real time over the Brazilian Amazon using Multitemporal fraction images derived from Terra MODIS', University of Maryland, 2005.
- [15]. H. Ferrufino Ugarte, T. Zawila-Niedzwiecki, J.R. Santos, F.D. Malonado, 'Change detection in the Amazon rainforest with radiometric rotation technique RCEN multi-spectral case study: Guarayos Bolivia', University of Applied Science Fh – Eberswalde – Forestry Faculty, Eberswalde – Brandenburg – Germany, 2007
- [16]. Yosio E. Shimabukuro, Valdete Duarte, Egidio Arai, Ramon M. Freitas, Paulo R. Martini and André Lima, 'Mapping and monitoring land cover in

Acre State, Brazilian Amazonia, using multitemporal remote sensing data',
2009

- [17]. Otsu segmentation method, Retrieved on August 15 2010, from
http://en.wikipedia.org/wiki/Otsu%27s_method
- [18]. Lab color space – definition, Retrieved on August 15 2010, from
http://www.wordiq.com/definition/Lab_color_space
- [19]. Earth observatory, NASA images , Retrieved on September 11 2010, from
<http://earthobservatory.nasa.gov/>
- [20]. Rodonia, Brazil, Retrieved on February 15, 2010, from
<http://en.wikipedia.org/wiki/Rond%C3%B4nia>
- [21]. Unsupervised image clustering, Retrieved on September 14, 2010, from
http://www.eng.tau.ac.il/research/laboratories/mip_lab/image_clustering.htm
- [22]. M. Ameer Ali, Gour C Karmakar and Laurence S Dooley, 'image segmentation using fuzzy clustering incorporating spatial information', Gippsland School of Computing & Information Technology, Monash University, Australia
- [23]. Fuzzy c-mean clustering, Retrieved on February 14, 2010, from
http://www.mathworks.de/products/fuzzylogic/demos.html?file=/products/demos/shipping/fuzzy/fcmdemo_codepad.html
- [24]. HSL and HSV color spaces, Retrieved on September 14, 2010, from
http://en.wikipedia.org/wiki/HSL_and_HSV

Appendix A

Image of Rondonia, Brazil (Source: U.S. geological survey, Images NASA)



Appendix B

```
%%%!%!%% HSI color space transformation code %%!%!%%

Image = imread('Image_to_be_HSI_transformed'); % Loading the image

X = Image;
XX = im2double(X);
r = XX(:, :, 1);
g = XX(:, :, 2);
b = XX(:, :, 3);

th = acos((0.5*((r-g)+(r-b)))/((sqrt((r-g).^2+(r-b).*(g-
b))+eps)));
H = th;
H(b>g) = 2*pi-H(b>g);
H = H/(2*pi);
S = 1-3.*(min(min(r,g),b))./(r + g + b +eps);
I = (r + g + b)/3;
ImHSI = cat(3,H,S,I); % HSI color space transformation

%%! extracting H, S and I channels %%!

H = ImHSI(:, :, 1); % H channel
S = ImHSI(:, :, 2); % S channel
I = ImHSI(:, :, 3); % I channel
```


Appendix C

```

%4.1.1 feature selection code %4.1.1.1 feature selection code %4.1.1.1
clear all
clc

Image = imread('Brazil_amazon.jpg');
rgbImage = Image;

%4.1.2 Color transformation to L*a*b* and HSV color spaces %4.1.2.1
rgbToLab = makecform('srgb2lab');
Lab = applycform(rgbImage, rgbToLab);

ImHsv = rgb2hsv(Image); % hsv color space transformation

%4.1.2.2 HSI color space transformation %4.1.2.2.1
X = Image;
XX = im2double(X);
r = XX(:, :, 1);
g = XX(:, :, 2);
b = XX(:, :, 3);
th = acos(((r-g)+(r-b))./(sqrt((r-g).^2+(r-b).*(g-
b)))+eps));
H = th;
H(b>g) = 2*pi-H(b>g);
H = H/(2*pi);
S = 1-3.*(min(min(r,g),b))./(r+g+b+eps);
I = (r+g+b)/3;
ImHSI = cat(3,H,S,I); % HSI color space transformation

%4.1.3 Extraction of 21 each channels of the color transformation
%4.1.3.1 L*a*b* channels
L = Lab(:, :, 1);
a = Lab(:, :, 2);
b = Lab(:, :, 3);

%4.1.3.2 hsv channels
h = ImHsv(:, :, 1);
s = ImHsv(:, :, 2);
v = ImHsv(:, :, 3);

%4.1.3.3 HSI channels
H = ImHSI(:, :, 1);
S = ImHSI(:, :, 2);
I = ImHSI(:, :, 3);

%4.1.4 Display the original image and the L*, a* and b* channels
figure,
subplot(221), imshow(rgbImage); title('Original Image');
subplot(222), imshow(L); title('L* channel');
subplot(223), imshow(a); title('a* channel');
subplot(224), imshow(b); title('b* channel');

%4.1.4 Display the original image and the h, s and v channels

```

```
figure,
subplot(221), imshow(rgbImage); title('Original Image');
subplot(222), imshow(h); title('h channel');
subplot(223), imshow(s); title('s channel');
subplot(224), imshow(v); title('v channel');
```

```
% Display the original image and the H, S and I channels
```

```
figure,
subplot(221), imshow(rgbImage); title('Original Image');
subplot(222), imshow(H); title('H channel');
subplot(223), imshow(S); title('S channel');
subplot(224), imshow(I); title('I channel');
```

```
% Apply Otsu method segmentation in the L*, a* and b* channels
```

```
level = graythresh(L);
binary= im2bw(L,level);
Segmented_L= imfill(binary,'holes'); % L* channel segmentation
```

```
level = graythresh(a);
binary= im2bw(a,level);
Segmented_a= imfill(binary,'holes'); % a* channel segmentation
```

```
level = graythresh(b);
binary= im2bw(b,level);
Segmented_b= imfill(binary,'holes'); % b* channel segmentation
```

```
% Display the original image and the transformed color space
images
```

```
figure,
subplot(221), imshow(rgbImage); title('Original Image');
subplot(222), imshow(Segmented_L); title('L* Segmented');
subplot(223), imshow(Segmented_a); title('a* Segmented');
subplot(224), imshow(Segmented_b); title('b* Segmented');
```

```
% Apply Otsu method segmentation in the h, s and v channels
```

```
level = graythresh(h);
binary= im2bw(h,level);
Segmented_h= imfill(binary,'holes'); % h channel segmentation
```

```
level = graythresh(s);
binary= im2bw(s,level);
Segmented_s= imfill(binary,'holes'); % s channel segmentation
```

```
level = graythresh(v);
binary= im2bw(v,level);
Segmented_v= imfill(binary,'holes'); % v channel segmentation
```

```
% Display the original image and the transformed color space
images
```

```
figure,
```

```

subplot(221), imshow(rgbImage); title('Original Image');
subplot(222), imshow(Segmented_h); title('h Segmented');
subplot(223), imshow(Segmented_s); title('s Segmented');
subplot(224), imshow(Segmented_v); title('v Segmented');

```

% Apply Otsu method segmentation in the h, s and v channels

```

level = graythresh(H);
binary= im2bw(H,level);
Segmented_H= imfill(binary, 'holes'); % H channel segmentation

```

```

level = graythresh(S);
binary= im2bw(S,level);
Segmented_S= imfill(binary, 'holes'); % S channel segmentation

```

```

level = graythresh(I);
binary= im2bw(I,level);
Segmented_I= imfill(binary, 'holes'); % V channel segmentation

```

% Display the original image and the transformed color space images

```

figure,
subplot(221), imshow(rgbImage); title('Original Image');
subplot(222), imshow(Segmented_H); title('H Segmented');
subplot(223), imshow(Segmented_S); title('S Segmented');
subplot(224), imshow(Segmented_I); title('I Segmented');

```



```

figure,
subplot(121), imshow(Image);
subplot(122), imshow(Segmented);

%%% Correlation + RMSE for accuracy assessment %%%

[m, n] = size (reference);

IM1 = reference;           % Manually segmented data
IM2 = IM_fcm;              % Otsu segmented data
Error = xor(IM1,IM2);      % Error
Error2 = sum(Error);
Total = sum (Error2);      % Total error

RMSE = Total / (m*n)

data=reshape(IM1,[],1);
datal=reshape(IM2,[],1);

```

Appendix E

```

clear all
clc

%FCM() based segmentation %FCM() based segmentation %FCM() based segmentation

Reference = imread ('Manual_segmented_image');

reference = im2bw(Reference);

Image = imread('Image to be segmented'); % Loading the image

%RGB to Lab and HSV color space transformations to Lab & HSV %RGB to Lab and HSV color space transformations to Lab & HSV %RGB to Lab and HSV color space transformations to Lab & HSV

rgbToLab = makecform('srgb2lab');
Lab = applycform(Image,rgbToLab); % lab color space transformation

ImHsv = rgb2hsv(Image); % hsv color space transformation

%HSV to HSI color space transformation %HSV to HSI color space transformation %HSV to HSI color space transformation

X = Image;
XX = im2double(X);
r = XX(:,:,1);
g = XX(:,:,2);
b = XX(:,:,3);
th = acos((0.5*((r-g)+(r-b)))/((sqrt((r-g).^2+(r-b).*(g-
b)))+eps));
H = th;
H(b>g) = 2*pi-H(b>g);
H = H/(2*pi);
S = 1-3.*(min(min(r,g),b))./(r+g+b+eps);
I = (r+g+b)/3;
ImHSI = cat(3,H,S,I); % HSI color space transformation

%Extract L,a,b & R,G,B & ,h,s,v & H,S,I components %Extract L,a,b & R,G,B & ,h,s,v & H,S,I components %Extract L,a,b & R,G,B & ,h,s,v & H,S,I components

L = Lab(:,:,1);
a = Lab(:,:,2);
b = Lab(:,:,3);

h = ImHsv(:,:,1);
s = ImHsv(:,:,2);
v = ImHsv(:,:,3);

H = ImHSI(:,:,1);
S = ImHSI(:,:,2);
I = ImHSI(:,:,3);

%FCM() based segmentation %FCM() based segmentation %FCM() based segmentation

IM = mat2gray(L); % manipulate L,V and I channels
data = reshape(IM, [], 1);

```

```

[center,member] = fcm(data,3,3);
[x, Level] = max(member,[],1);
IMout = reshape(center(Level), size(I));

figure, subplot(121), imshow(Image);
subplot(122), imshow(IM_fcm);

%% Correlation + RMSE for accuracy assessment %3-

[m, n] = size (reference);

IM1 = reference; % Manually segmented data
IM2 = IM_fcm; % fcm segmented data
Error = xor(IM1,IM2); % Error
Error2 = sum(Error);
Total = sum (Error2); % Total error

RMSE = Total / (m*n)

data=reshape(IM1,[],1);
data1=reshape(IM2,[],1);

Correlation = corr(data, data1) % Correlation

```

Appendix F

Rodonia, Brazil 1975

Original image



Fcm clustered

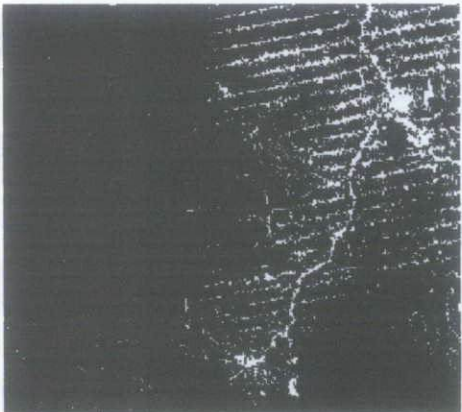


Rodonia, Brazil 1989

Original image



Fcm clustered



Rodonia, Brazil 2001

Original image



Fcm clustered



Amazon, Brazil 2003

Original image

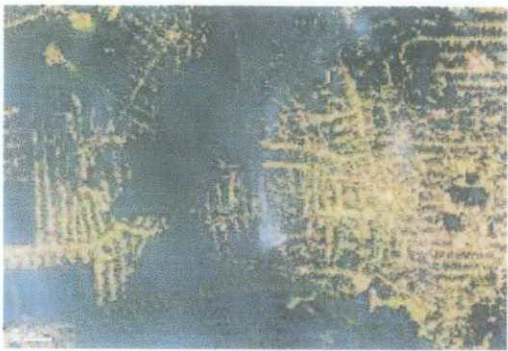


Fcm clustered

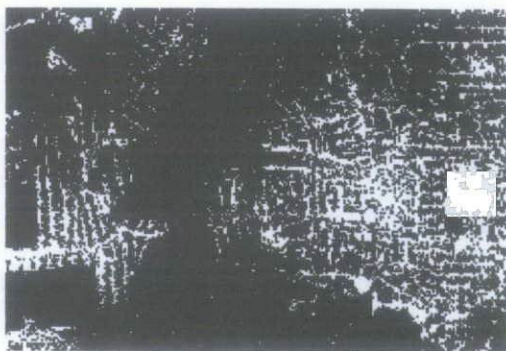


Amazon, Brazil 2004

Original image

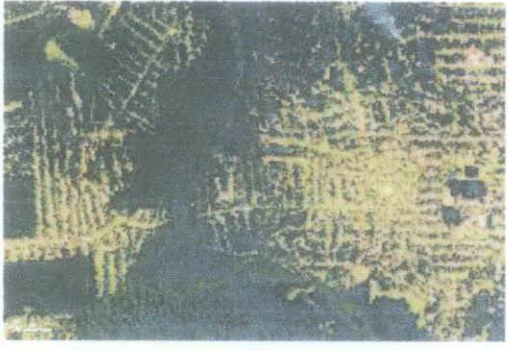


Fcm clustered

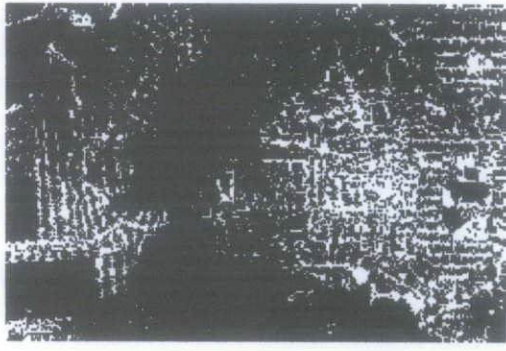


Amazon, Brazil 2005

Original image

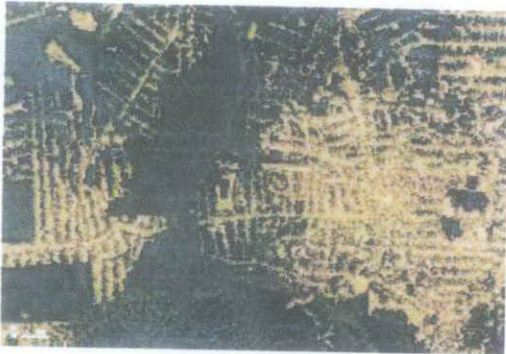


Fcm clustered

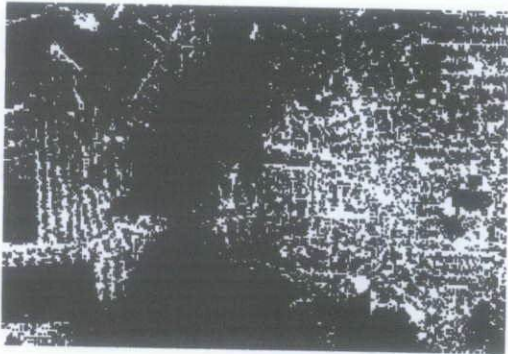


Amazon, Brazil 2006

Original image

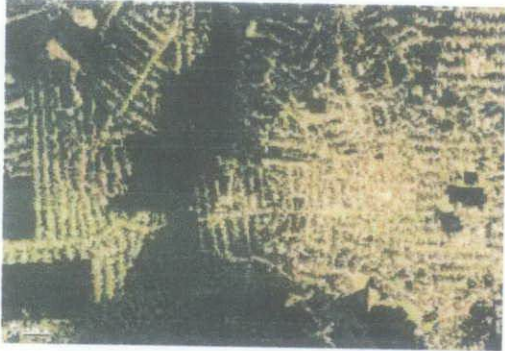


Fcm clustered

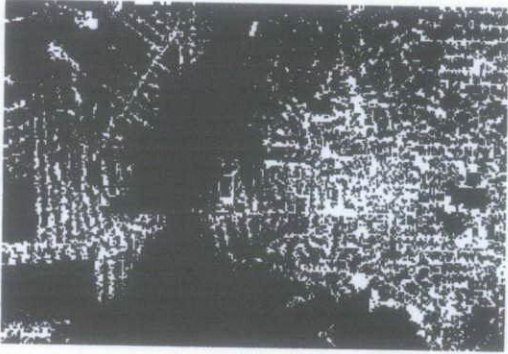


Amazon, Brazil 2008

Original image



Fcm clustered



Amazon, Brazil 2009

Original image



Fcm clustered

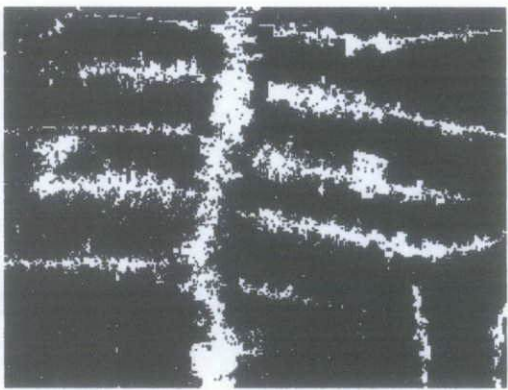


Amazon, Brazil

Original image

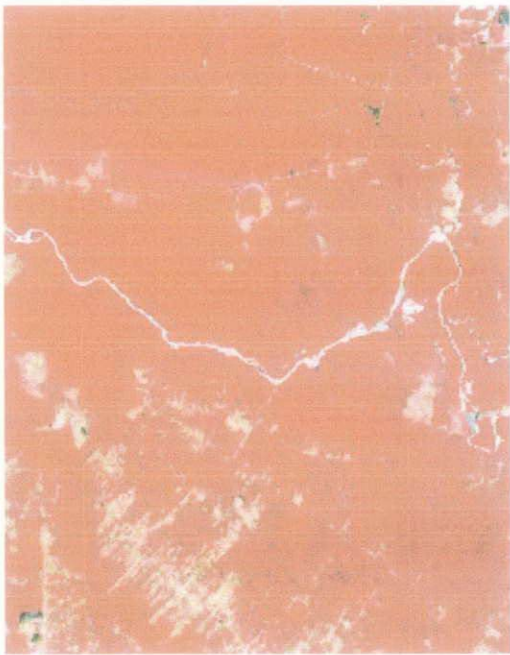


Fcm clustered



Matogrosso

Original image



Fcm clustered



Appendix G

```

%% deforested area under fcm clustering %300x4

clear all
clc

%% 300x400x3, Segmentation based on GTSU on image one %300x400x3

Manual_1975 = imread('1975bw.png');
Manual_1989 = imread('1989bw.png');
Manual_2001 = imread('2001bw.png');

Reference_1975 = im2bw(Manual_1975);
Reference_1989 = im2bw(Manual_1989);
Reference_2001 = im2bw(Manual_2001);

Image_1975 = imread('1975.png');
Image_1989 = imread('1989.png');
Image_2001 = imread('2001.png');

rgbImage_1975 = Image_1975;
rgbImage_1989 = Image_1989;
rgbImage_2001 = Image_2001;

%% Create transformation function from RGB to Lab space

rgbToLab_1975 = makecform('srgb2lab');
Lab_1975 = applycform(rgbImage_1975,rgbToLab_1975);

rgbToLab_1989 = makecform('srgb2lab');
Lab_1989 = applycform(rgbImage_1989,rgbToLab_1989);

rgbToLab_2001 = makecform('srgb2lab');
Lab_2001 = applycform(rgbImage_2001,rgbToLab_2001);

%% HSI color space transformation %300x400x3x3

X_1 = Image_1975;
XX_1 = im2double(X_1);
r_1 = XX_1(:,:,1);
g_1 = XX_1(:,:,2);
b_1 = XX_1(:,:,3);
th_1 = acos((0.5*((r_1-g_1)+(r_1-b_1)))/((sqrt((r_1-g_1).^2+(r_1-
b_1).*(g_1-b_1)))+eps));
H_1 = th_1;
H_1(b_1>g_1) = 2*pi-H_1(b_1>g_1);
H_1 = H_1/(2*pi);
S_1 = 1-3.*(min(min(r_1,g_1),b_1))./(r_1+g_1+b_1+eps);
I_1 = (r_1+g_1+b_1)/3;
ImHSI_1975 = cat(3,H_1,S_1,I_1); % HSI color space
transformation

X_2 = Image_1989;
XX_2 = im2double(X_2);

```



```

r_2 = XX_2(:, :, 1);
g_2 = XX_2(:, :, 2);
b_2 = XX_2(:, :, 3);
th_2 = acos((0.5*((r_2-g_2)+(r_2-b_2)))/((sqrt((r_2-g_2).^2+(r_2-
b_2).*(g_2-b_2)))+eps));
H_2 = th_2;
H_2(b_2>g_2) = 2*pi-H_2(b_2>g_2);
H_2 = H_2/(2*pi);
S_2 = 1-3.*(min(min(r_2,g_2),b_2))./(r_2+g_2+b_2+eps);
I_2 = (r_2+g_2+b_2)/3;
ImHSI_1989 = cat(3,H_2,S_2,I_2);           % HSI color space
transformation

```

```

X_3 = Image_2001;
XX_3 = im2double(X_3);
r_3 = XX_3(:, :, 1);
g_3 = XX_3(:, :, 2);
b_3 = XX_3(:, :, 3);
th_3 = acos((0.5*((r_3-g_3)+(r_3-b_3)))/((sqrt((r_3-g_3).^2+(r_3-
b_3).*(g_3-b_3)))+eps));
H_3 = th_3;
H_3(b_3>g_3) = 2*pi-H_3(b_3>g_3);
H_3 = H_3/(2*pi);
S_3 = 1-3.*(min(min(r_3,g_3),b_3))./(r_3+g_3+b_3+eps);
I_3 = (r_3+g_3+b_3)/3;
ImHSI_2001 = cat(3,H_3,S_3,I_3);          % HSI color space
transformation

```

```

ImHsv_1975 = rgb2hsv(Image_1975);         % hsv color space
transformation
ImHsv_1989 = rgb2hsv(Image_1989);         % hsv color space
transformation
ImHsv_2001 = rgb2hsv(Image_2001);         % hsv color space
transformation

```

```

% Extract L, a, b components from the 3 images

```

```

L_1975 = Lab_1975(:, :, 1);
a_1975 = Lab_1975(:, :, 2);
b_1975 = Lab_1975(:, :, 3);

```

```

L_1989 = Lab_1989(:, :, 1);
a_1989 = Lab_1989(:, :, 2);
b_1989 = Lab_1989(:, :, 3);

```

```

L_2001 = Lab_2001(:, :, 1);
a_2001 = Lab_2001(:, :, 2);
b_2001 = Lab_2001(:, :, 3);

```

```

h_1975 = ImHsv_1975(:, :, 1);
s_1975 = ImHsv_1975(:, :, 2);
v_1975 = ImHsv_1975(:, :, 3);

```

```

h_1989 = ImHsv_1989(:,:,1);
s_1989 = ImHsv_1989(:,:,2);
v_1989 = ImHsv_1989(:,:,3);

h_2001 = ImHsv_2001(:,:,1);
s_2001 = ImHsv_2001(:,:,2);
v_2001 = ImHsv_2001(:,:,3);

H_1975 = ImHSI_1975(:,:,1);
S_1975 = ImHSI_1975(:,:,2);
I_1975 = ImHSI_1975(:,:,3);

H_1989 = ImHSI_1989(:,:,1);
S_1989 = ImHSI_1989(:,:,2);
I_1989 = ImHSI_1989(:,:,3);

H_2001 = ImHSI_2001(:,:,1);
S_2001 = ImHSI_2001(:,:,2);
I_2001 = ImHSI_2001(:,:,3);

%% fcm clustering and segmentation

IM_1975 = mat2gray(L_1975);
data_1975 = reshape(IM_1975,[],1);
[center_1975,member_1975] = fcm(data_1975,12);
[x_1975, Level_1975] = max(member_1975,[],1);
IMout_1975 = reshape(center_1975(Level_1975), size(L_1975));

IM_1975_fcm = im2bw (IMout_1975);

IM_1989 = mat2gray(L_1989);
data_1989 = reshape(IM_1989,[],1);
[center_1989,member_1989] = fcm(data_1989,3,3);
[x_1989, Level_1989] = max(member_1989,[],1);
IMout_1989 = reshape(center_1989(Level_1989), size(L_1989));

IM_1989_fcm = im2bw (IMout_1989);

IM_2001 = mat2gray(L_2001);
data_2001 = reshape(IM_2001,[],1);
[center_2001,member_2001] = fcm(data_2001,3,3);
[x_2001, Level_2001] = max(member_2001,[],1);
IMout_2001 = reshape(center_2001(Level_2001), size(L_2001));

IM_2001_fcm = im2bw (IMout_2001);

%% AREA CALCULATION OF THE DEFORESTED AREA ~~~~~~

[m1,n1] = size(IM_1975_fcm);
[m2,n2] = size(IM_1989_fcm);
[m3,n3] = size(IM_2001_fcm);

% Built in function area %
total_1 = bwarea(IM_1975_fcm);
Area_1975 = total_1/(m1*n1)

```

```
total_2 = bwarea(IM_1989_fcm);
Area_1989 = total_2/(m2*n2)
```

```
total_3 = bwarea(IM_2001_fcm);
Area_2001 = total_3/(m3*n3)
```

```
% Show the result of all the year segmentation VS the original
image
```

```
figure,
subplot(231), imshow(rgbImage_1975); title('1975 Image');
subplot(234), imshow(IM_1975_fcm); title('1975 Segmented');
subplot(232), imshow(rgbImage_1989); title('1989 Image');
subplot(235), imshow(IM_1989_fcm); title('1989 Segmented');
subplot(233), imshow(rgbImage_2001); title('2001 Image');
subplot(236), imshow(IM_2001_fcm); title('2001 Segmented');
```

```
% 1975 result alone
```

```
figure,
subplot(121), imshow(rgbImage_1975); title('1975 Image');
subplot(122), imshow(IM_1975_fcm); title('1975 Segmented');
```

```
% 1989 result alone
```

```
figure,
subplot(121), imshow(rgbImage_1989); title('1989 Image');
subplot(122), imshow(IM_1989_fcm); title('1989 Segmented');
```

```
% 2001 result alone
```

```
figure,
subplot(121), imshow(rgbImage_2001); title('2001 Image');
subplot(122), imshow(IM_2001_fcm); title('2001 Segmented');
```

Appendix H

Fuzzy C-mean Clustering results

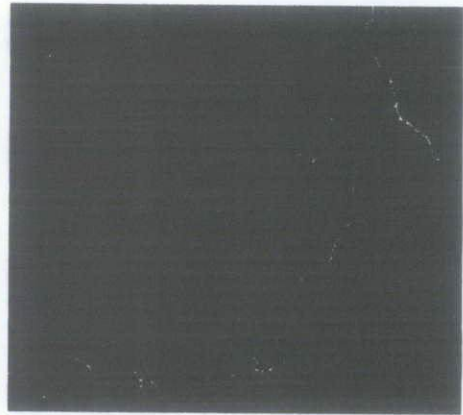


Figure a: 1975 L* channel fcm segmented

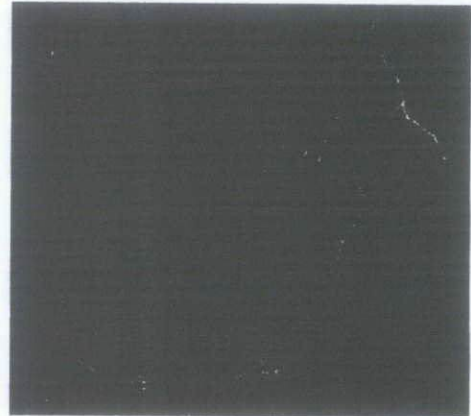


Figure b: 1975 I channel fcm segmented

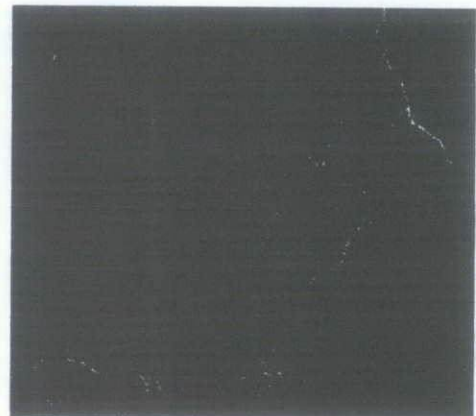


Figure c: 1975 V channel fcm segmented

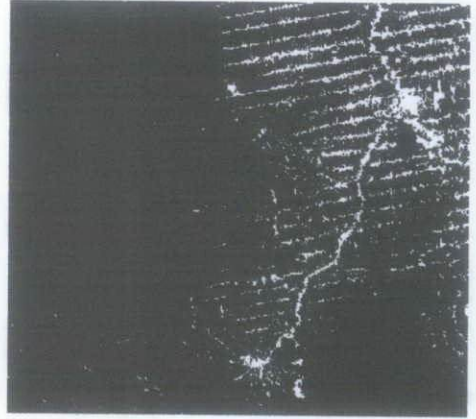


Figure d: 1989 L* channel fcm segmented

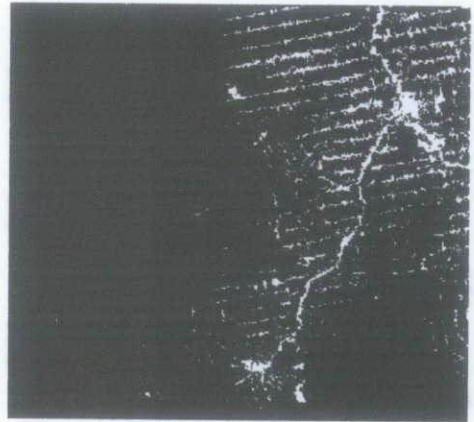


Figure e: 1989 I channel fcm segmented

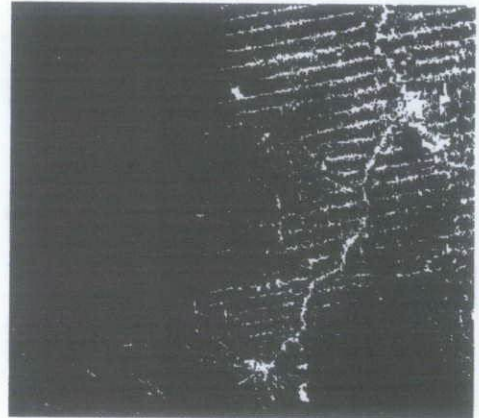


Figure f: 1989 V channel fcm segmented

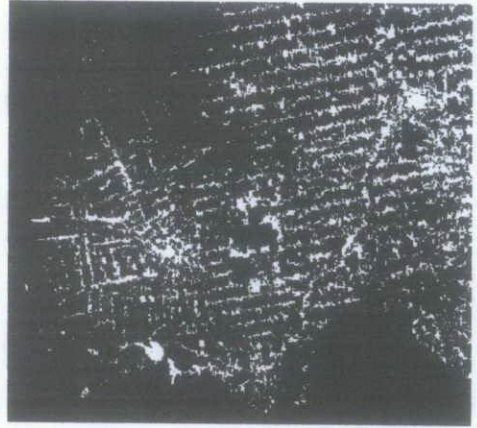


Figure g: 2001 L* channel fcm segmented

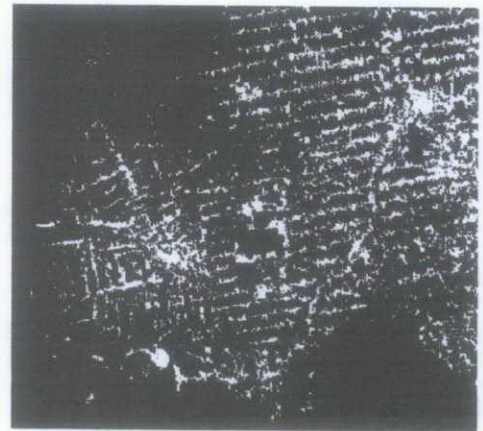


Figure h: 2001 I channel fcm segmented

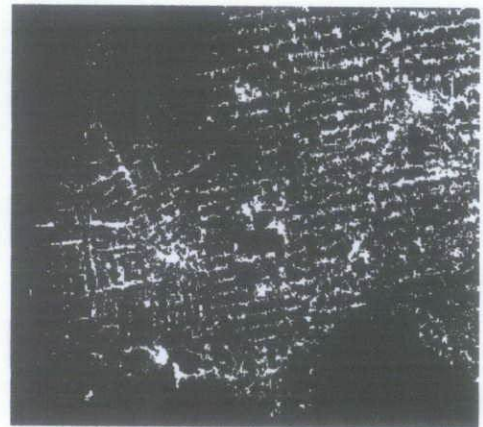


Figure i: 2001 V channel fcm segmented

OTSU segmentation results

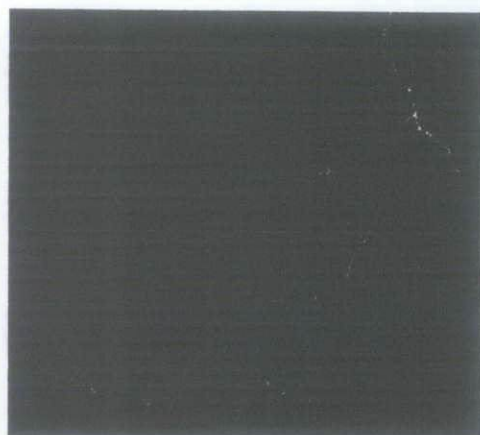


Figure j: 1975 L* channel OTSU segmented

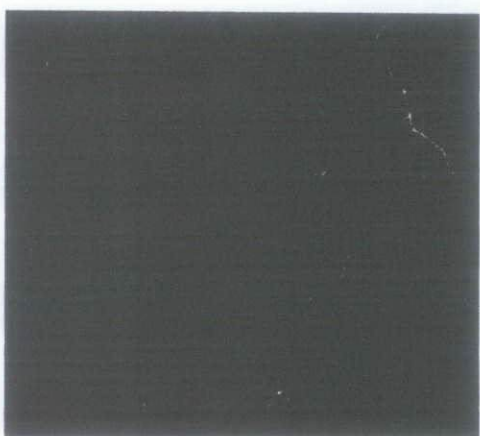


Figure k: 1975 I channel OTSU segmented

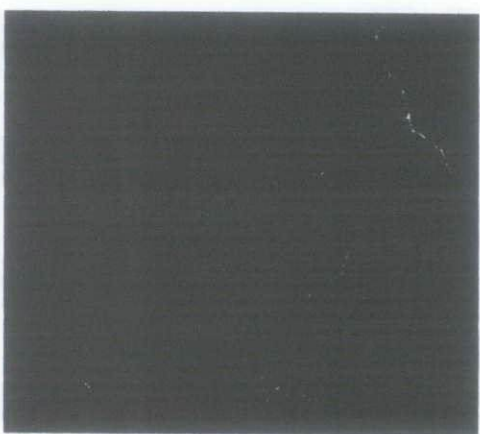


Figure l: 1975 V channel OTSU segmented

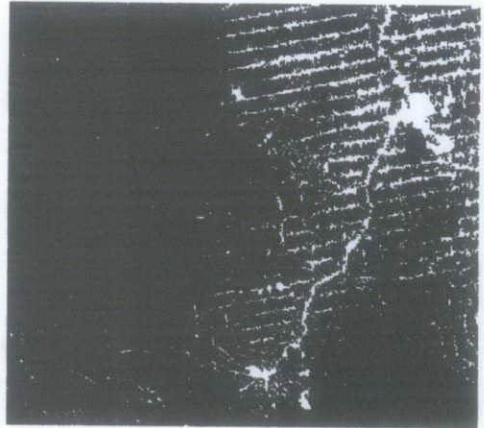


Figure m: 1989 L* channel OTSU segmented

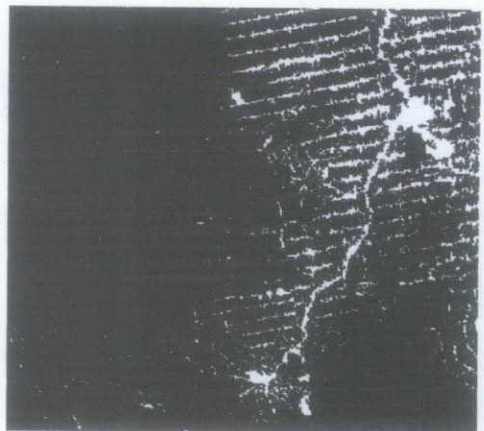


Figure n: 1989 I channel OTSU segmented

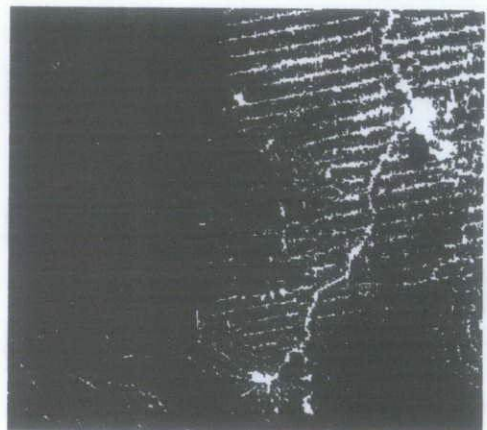


Figure o: 1989 V channel OTSU segmented



Figure p: 2001 V channel OTSU segmented

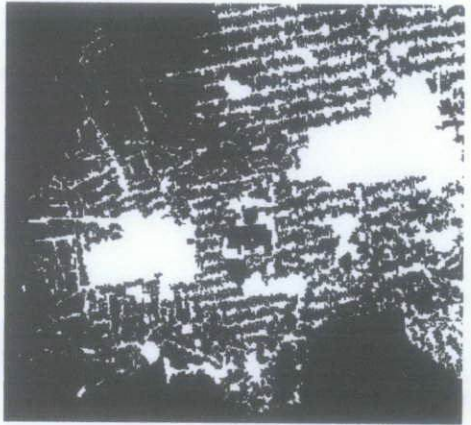


Figure q: 2001 I channel OTSU segmented



Figure r: 2001 V channel OTSU segmented